

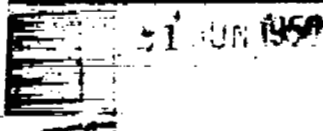
CONFIDENTIAL

UNCLASSIFIED

Copy
RM L50D21

5

NACA RM L50D21



41255
NACA/32

NACA

RESEARCH MEMORANDUM

INVESTIGATION OF THE NACA 3-(3)(05)-05 EIGHT-BLADE
DUAL-ROTATING PROPELLER AT FORWARD MACH
NUMBERS TO 0.925

By Robert J. Platt, Jr. and Robert A. Shumaker

Langley Aeronautical Laboratory
Langley Air Force Base, Va.

CLASSIFICATION CANCELLED

CLASSIFIED DOCUMENT

Author: NACA R 7 2529 Date 8/13/54
By: MAA 9/7/54 See _____

This document contains classified information in accordance with the Espionage Act, 18 USC 793 and 794. Its transmission or the revelation of its contents in any manner to an unauthorized person is prohibited by law. Information so classified may be imparted only to persons in the military and naval services of the United States, appropriate civilian officers and employees of the Federal Government who have a legitimate interest therein, and to United States citizens of known loyalty and discretion who of necessity must be informed thereof.

LANGLEY AERONAUTICAL LABORATORY

NATIONAL ADVISORY COMMITTEE FOR AERONAUTICS

WASHINGTON
June 19, 1950

CONFIDENTIAL

ENCLOSURE

UNCLASSIFIED

NACA RM L50D21

~~CONFIDENTIAL~~

NATIONAL ADVISORY COMMITTEE FOR AERONAUTICS

RESEARCH MEMORANDUM

INVESTIGATION OF THE NACA 3-(3)(05)-05 EIGHT-BLADE
DUAL-ROTATING PROPELLER AT FORWARD MACH
NUMBERS TO 0.925

By Robert J. Platt, Jr. and Robert A. Shumaker

SUMMARY

Force tests were made on an NACA 3-(3)(05)-05 eight-blade dual-rotating propeller in the Langley 8-foot high-speed tunnel. The tests covered a blade-angle range from 55° to 80° at forward Mach numbers to 0.925.

The results indicate that good efficiencies can be obtained at high subsonic forward Mach numbers by operation at high blade angles; at a front-propeller blade-angle setting of 75° , the maximum efficiency was 87 percent at a Mach number of 0.80, and 79 percent at a Mach number of 0.85. Little or no efficiency gain could be realized by increasing the blade angle beyond 75° .

INTRODUCTION

The NACA is conducting a general investigation to study the effects of compressibility, design camber, blade sweep, thickness ratio, and dual rotation on propeller performance at transonic speeds. Results of the first two phases of this investigation, dealing with the effects of compressibility and design camber on performance, were presented in references 1 and 2; blade sweep, in references 3 and 4; and thickness ratio, in references 5 and 6.

Several investigations have been made to study the effect of dual rotation on propeller performance, but all have been limited to low forward Mach numbers. Results of these investigations show that the maximum efficiency of a dual-rotating propeller is greater than that of a comparable single-rotating propeller at high values of advance ratio (references 7 and 8). This gain in efficiency can be attributed to the much smaller slipstream rotation losses of the dual propeller.

~~CONFIDENTIAL~~

UNCLASSIFIED

The results of reference 9 indicate that the induced losses of a dual propeller are relatively independent of blade load distribution. A dual propeller therefore could be designed to carry, without loss of efficiency, a greater load on the inboard sections and a smaller load on the outboard sections than would be required for an optimum single-rotating propeller. Such a dual propeller, operated at a high advance ratio, should be well suited for operation at high subsonic forward Mach numbers, since both the lower rotational speed and reduced outboard loading would tend to delay the compressibility loss. A propeller of this type has been designed and tested by the NACA in the Langley 8-foot high-speed tunnel.

Presented herein are the force-test results for the NACA 3-(3)(05)-05 eight-blade dual-rotating propeller for blade angles from 55° to 80° at forward Mach numbers to 0.925. Only a limited analysis of the force-test results is presented at this time to expedite publication of the basic propeller results. Large-scale plots of the basic propeller characteristics (figs. 6 and 7) are available on request to the NACA.

SYMBOLS

b blade section chord, feet

c_l section lift coefficient

c_{l_d} design lift coefficient

C_P total power coefficient $\left(\frac{P}{\rho n_F^3 D^5} \right)$

C_{P_F} front power coefficient $\left(\frac{P_F}{\rho n_F^3 D^5} \right)$

C_{P_R} rear power coefficient $\left(\frac{P_R}{\rho n_R^3 D^5} \right)$

- C_{P_R} rear power coefficient $\left(\frac{P_R}{\rho n_F^3 D^5} \right)$
- C_T total thrust coefficient $\left(\frac{T}{\rho n_F^2 D^4} \right)$
- D propeller diameter, feet
- h maximum thickness of blade section, feet
- J advance ratio $\left(\frac{V_O}{nD} \right)$
- M tunnel datum (forward) Mach number (tunnel Mach number uncorrected for tunnel-wall constraint)
- M_{t_F} helical-tip Mach number of front propeller $\left(M \sqrt{1 + \frac{\pi^2}{J_F^2}} \right)$
- n propeller rotational speed, rps
- P power absorbed by propeller, foot-pounds per second
- q dynamic pressure, pounds per square foot $\left(\frac{\rho V^2}{2} \right)$
- R radius to propeller tip, feet
- T thrust, pounds
- T_c thrust disc-loading coefficient $\left(\frac{T}{2qD^2} \right)$
- V tunnel-datum velocity (tunnel velocity uncorrected for tunnel-wall constraint), feet per second
- V_O equivalent free-air velocity (tunnel-datum velocity corrected for tunnel-wall constraint), feet per second

β section blade angle, degrees
 $\beta_{0.75R}$ section blade angle at 0.75 tip radius, degrees

η efficiency $\left(\frac{J_F C_T}{C_P} \right)$

η_{\max} maximum efficiency

ρ air density, slugs per cubic foot

Subscripts:

F front propeller

R rear propeller

APPARATUS

Test equipment.- The propeller dynamometer described in reference 1 was modified to permit a dual propeller to be tested. These modifications consisted of the removal of the flexible coupling between the drive shafts of the two dynamometer units, the addition of a thrust-measuring unit to the front dynamometer, and the addition of a tachometer to permit the measurement of the rotational speed of each propeller. A sketch of the 800-horsepower propeller dynamometer, which was installed in the Langley 8-foot high-speed tunnel, is shown in figure 1.

The variable-frequency power required to drive the four dynamometer motors was obtained from a single motor-generator set. Therefore, differences in loading between the front and rear propellers, coupled with differences in the motor characteristics, resulted in unequal rotational speeds of the two propellers. This difference in rotational speed amounted to a maximum of 1.7 percent.

Propeller.- The 3-foot-diameter dual-rotating propeller consisted of eight blades: four in the front propeller and four of opposite hand in the rear propeller. A large spinner with a diameter 36 percent of the propeller diameter was used. The distance between the propeller center lines was 6 inches.

The front and rear blades differed slightly in twist, as shown by the blade-form curves of figure 2. In other respects the design of the

front and rear blades was identical. NACA 16-series airfoil sections were used throughout. A photograph of a blade is shown in figure 3. The offset of the blade at the root was intended to counteract the torque-force bending moment at the high blade angle for which the propeller was designed.

The propeller was designed for an advance ratio of 7.15 and a total power coefficient of 6.48. The tip Mach number at such a high advance ratio was only about 9 percent greater than the forward Mach number. The design blade angle of the propeller was approximately 75° .

The blade loading for which the eight-blade dual propeller was designed is shown in figure 4. Also shown for comparison is the minimum induced-energy-loss loading of an eight-blade single-rotating propeller at the same advance ratio of 7.15. It is evident that the dual propeller was designed to carry more load on the inboard blade sections and less load outboard than would be carried by a single-rotating propeller of minimum induced energy loss.

TESTS

Each run was made at a fixed value of tunnel Mach number and blade-angle setting, with the rotational speed varied to cover a range of advance ratio. The difference in blade angle between the front and rear propellers was chosen to produce approximately equal power absorption at

peak efficiency. The range of blade angle and Mach number covered is given in the following table:

Forward Mach number, M	Blade angle at 0.75R (deg)											
	β_F	β_R	β_F	β_R	β_F	β_R	β_F	β_R	β_F	β_R	β_F	β_R
0.35	--	----	60	58.5	65	63.3	70	68.2	75	73	--	----
.53	--	----	60	58.5	65	63.3	70	68.2	75	73	80	77.8
.60	55	53.7	60	58.5	65	63.3	70	68.2	75	73	80	77.8
.65	55	53.7	60	58.5	65	63.3	70	68.2	75	73	80	77.8
.70	55	53.7	60	58.5	65	63.3	70	68.2	75	73	80	77.8
	--	----	60	60	--	----	--	----	75	75	--	----
	--	----	--	----	--	----	--	----	75	73.5	--	----
	--	----	--	----	--	----	--	----	75	72	--	----
.75	55	53.7	60	58.5	65	63.3	70	68.2	75	73	80	77.8
.80	--	----	60	58.5	65	63.3	70	68.2	75	73	80	77.8
.85	--	----	60	58.5	65	63.3	70	68.2	75	73	80	77.8
	--	----	60	60	--	----	--	----	--	----	--	----
.90	--	----	--	----	65	63.3	70	68.2	75	73	80	77.8
	--	----	--	----	--	----	--	----	75	75	--	----
	--	----	--	----	--	----	--	----	75	73.5	--	----
	--	----	--	----	--	----	--	----	75	72	--	----
.925	--	----	--	----	65	63.3	70	68.2	75	73	80	77.8

REDUCTION OF DATA

Propeller thrust.- The determination of the separate thrusts of front and rear propellers would have required the measurement of the pressure existing between the front and rear spinners at each operating condition. An attempt to measure this pressure with electrical pressure pickups proved unsuccessful; therefore, only the over-all thrust could be determined. Propeller thrust as used herein is defined as the sum

of the two axial shaft forces produced by the spinner-to-tip portion of the blades. The method used to determine thrust tares and evaluate the propeller thrust is similar to that used for a single-rotating propeller as described in reference 1.

Propeller torque.- The indicated torques of the front and rear propellers were corrected for spinner tares. These corrections were small and dependent only on rotational speed.

Tunnel-wall correction.- The data (except for Mach number) have been corrected for the effect of tunnel-wall constraint on velocity at the propeller test plane by the theory of reference 10. This velocity correction is shown in figure 5. A few experimental checks of this correction were made by the method of reference 1; good agreement was obtained.

RESULTS AND DISCUSSION

The over-all propeller characteristics are presented in figure 6 for each test value of tunnel-datum Mach number. The total thrust coefficient C_T and total power coefficient C_P are based on the front-propeller rotational speed. These coefficients and the efficiency are plotted against the advance ratio of the front propeller. The variation of the front-propeller tip Mach number with its advance ratio is included in the figure. As used herein, the tunnel-datum Mach number M is not corrected for tunnel-wall constraint. The free-air Mach number, however, can be obtained by applying the velocity correction, presented in figure 5, to the tunnel-datum Mach number. The correction will be a maximum at a tunnel-datum Mach number of 0.925, a blade angle of 65° , and an advance ratio of 3.85. At this point, the correction to the Mach number is 1.2 percent and the free-air Mach number becomes 0.914.

The individual power coefficients of the dual propeller are shown in figure 7. The front-propeller power coefficient C_{P_F} is based on the front-propeller rotational speed n_F and plotted against the front-propeller advance ratio J_F . The rear-propeller power coefficient is shown in two forms: C_{P_R} is based on n_R and plotted against J_R ; whereas C_{P_R}' is based on n_F and plotted against J_F . The relation

between the total power coefficient presented in figure 6 and the individual power coefficients presented in figure 7 is

$$C_P = C_{P_F} + C_{P_R}$$

The effect of forward Mach number on the maximum efficiency of the dual propeller is shown in figure 8 for several blade angles. At low Mach numbers the maximum efficiency is about 90 percent for front-propeller blade-angle settings from 65° to 75° . The relatively low efficiency of about 85 percent at the highest test blade angle of 80° is probably the result of an unfavorable geometry of the force vectors, which tends to magnify the effect of profile drag.

As has been shown previously for single-rotating propellers, increasing the blade angle delays to higher Mach numbers the efficiency loss due to compressibility effects. The results show, however, that little or no efficiency gain can be realized by increasing the front-propeller blade-angle setting beyond 75° . For a front propeller blade-angle setting of 75° , which is very near the design angle, the maximum efficiency is 87 percent at a Mach number of 0.80 and 79 percent at a Mach number of 0.85. Operation of a propeller at such a high blade angle entails, however, a reduction in the power which can be absorbed. This, of course, is a result of the low rotational speed of the propeller.

The maximum efficiency is plotted in figure 9 against the front-propeller advance ratio J_F for each test value of forward Mach number. Good efficiencies are obtained at high values of advance ratio up to forward Mach numbers as high as 0.85. At the highest test Mach numbers of 0.90 and 0.925, the data indicate that operation at lower values of advance ratio is necessary for best efficiency. This effect is similar to that previously found for single-rotating propellers.

The effect of small changes in the rear-propeller blade angle on the dual-propeller characteristics is shown in figure 10 for a front blade angle of 75° . At a Mach number of 0.70 there is no measurable change in front-propeller power coefficient for the range of rear-propeller blade angles investigated. However, at the supercritical Mach number of 0.90, the rear propeller does influence the front-propeller power absorption; a decrease in the rear-propeller blade angle causes a slight increase in the front-propeller power coefficient.

More limited data of a similar type are shown in figure 11 for a front-propeller blade angle of 60° . The rear propeller appears to have little influence on the front-propeller power coefficient at a Mach number of 0.70. However, at the high supercritical Mach number of 0.85, its effect is pronounced.

The differences in maximum over-all efficiency at the various rear-propeller blade-angle settings, shown in figures 10 and 11, are believed to be within the experimental accuracy.

CONCLUSIONS

Force-test results for the NACA 3-(3)(05)-05 eight-blade dual propeller at Mach numbers to 0.925 indicated the following conclusions:

1. Good efficiencies were obtained at high subsonic forward Mach numbers by operation at high blade angles; at a front-propeller blade-angle setting of 75° , the maximum efficiency was 87 percent at a Mach number of 0.80 and 79 percent at a Mach number of 0.85.
2. Little or no efficiency gain could be realized by increasing the blade angle beyond 75° .

Langley Aeronautical Laboratory
National Advisory Committee for Aeronautics
Langley Air Force Base, Va.

REFERENCES

1. Delano, James B., and Carmel, Melvin M.: Investigation of the NACA 4-(5)(08)-03 Two-Blade Propeller at Forward Mach Numbers to 0.925. NACA RM L9G06a, 1949
2. Delano, James B., and Morgan, Francis G., Jr.: Investigation of the NACA 4-(3)(08)-03 Two-Blade Propeller at Forward Mach Numbers to 0.925. NACA RM L9I06, 1949.
3. Delano, James B., and Harrison, Daniel E.: Investigation of the NACA 4-(4)(06)-04 Two-Blade Propeller at Forward Mach Numbers to 0.925. NACA RM L9I07, 1949.
4. Delano, James B., and Harrison, Daniel E.: Investigation of the NACA 4-(4)(06)-057-45A and NACA 4-(4)(06)-057-45B Two-Blade Swept Propellers at Forward Mach Numbers to 0.925. NACA RM L9L05, 1950.
5. Delano, James B., and Carmel, Melvin M.: Investigation of NACA 4-(0)(03)-045 and NACA 4-(0)(08)-045 Two-Blade Propellers at Forward Mach Numbers to 0.925. NACA RM L9L06a, 1950.
6. Carmel, Melvin M., and Milillo, Joseph R.: Investigation of the NACA 4-(0)(03)-045 Two-Blade Propeller at Forward Mach Numbers to 0.925. NACA RM L50A31a, 1950.
7. Biermann, David, and Hartman, Edwin P.: Wind-Tunnel Tests of Four- and Six-Blade Single- and Dual-Rotating Tractor Propellers. NACA Rep. 747, 1942.
8. Lesley, E. P.: Tandem Air Propellers - II. NACA TN 822, 1941.
9. Gilman, Jean, Jr.: Wind-Tunnel Tests and Analysis of Two 10-Foot-Diameter Six-Blade Dual-Rotating Tractor Propellers Differing in Pitch Distribution. NACA TN 1634, 1948.
10. Young, A. D.: Note on the Application of the Linear Perturbation Theory to Determine the Effect of Compressibility on Wind Tunnel Constraint on a Propeller. RAE TN No. Aero. 1539, Nov. 1944. (Also available as R. & M. No. 2113, British A.R.C., 1944.)

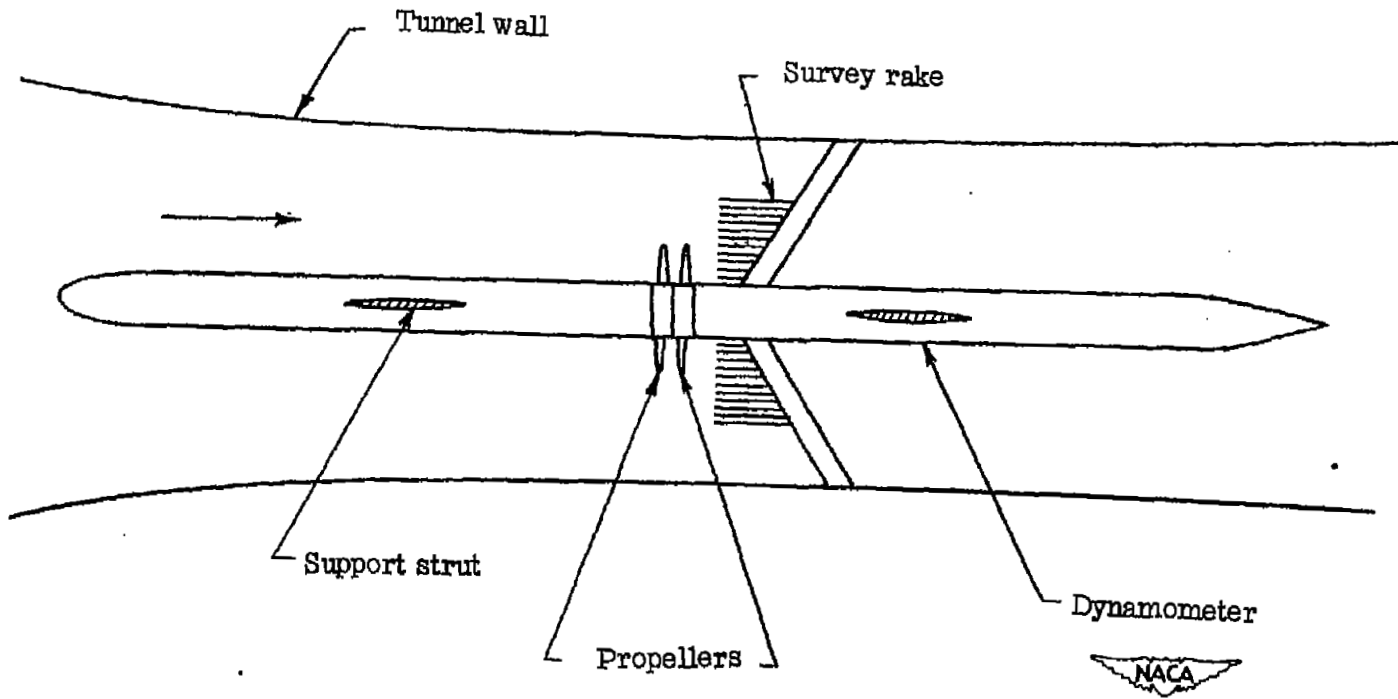


Figure 1.- Test apparatus.



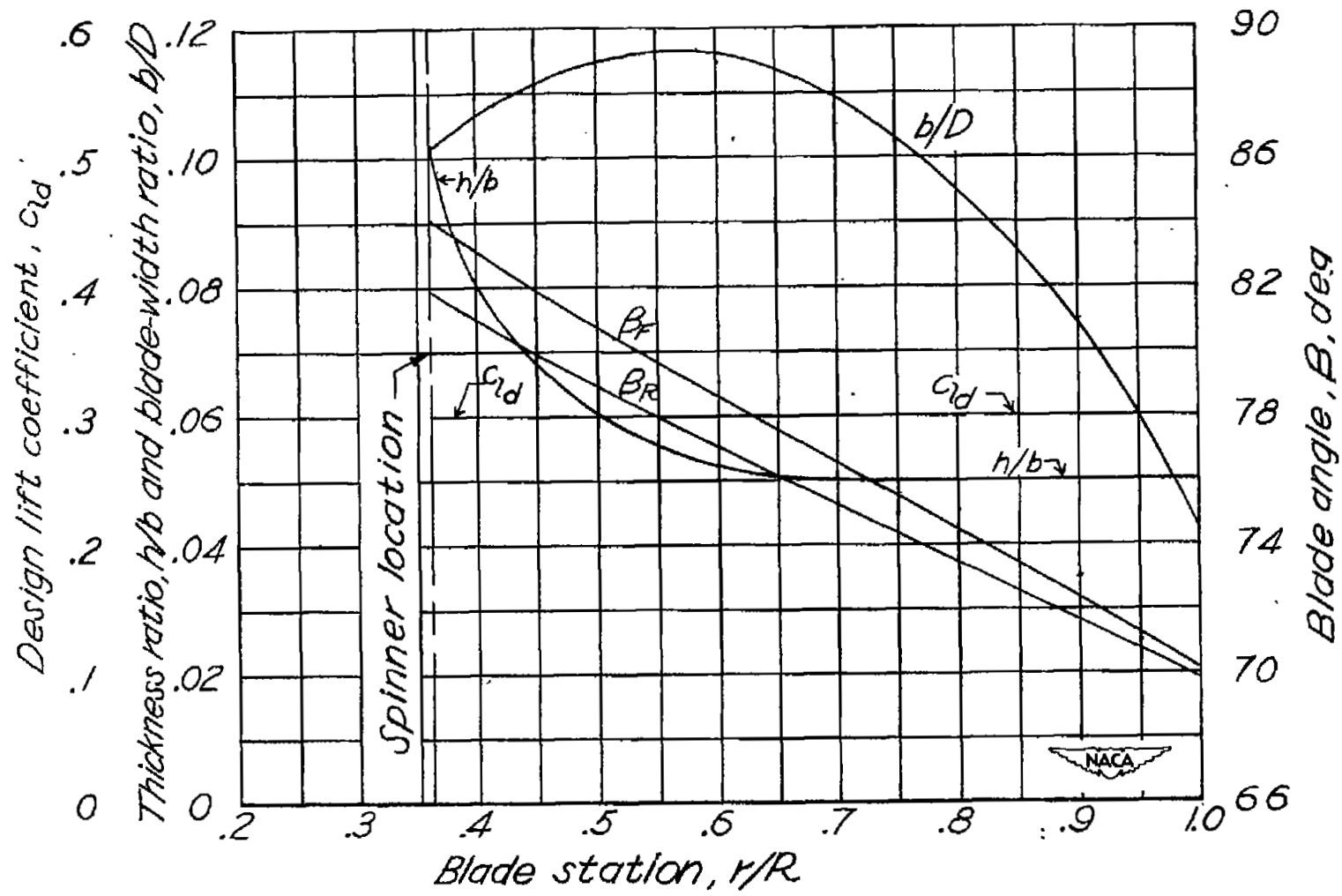


Figure 2.- Blade-form curves for NACA 3-(3)(05)-05 dual propeller.

Twist factor = 1 + 3 per line

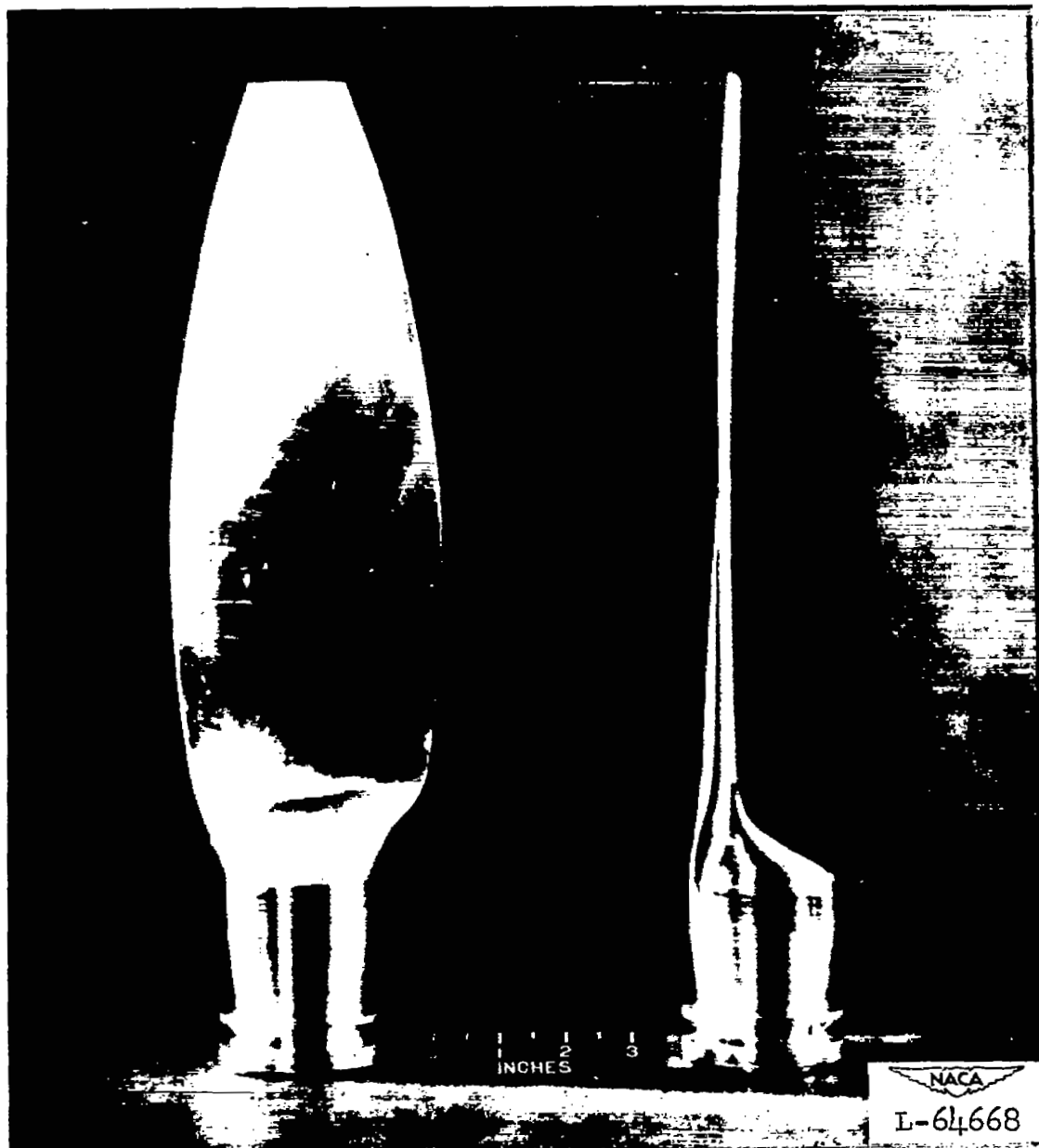
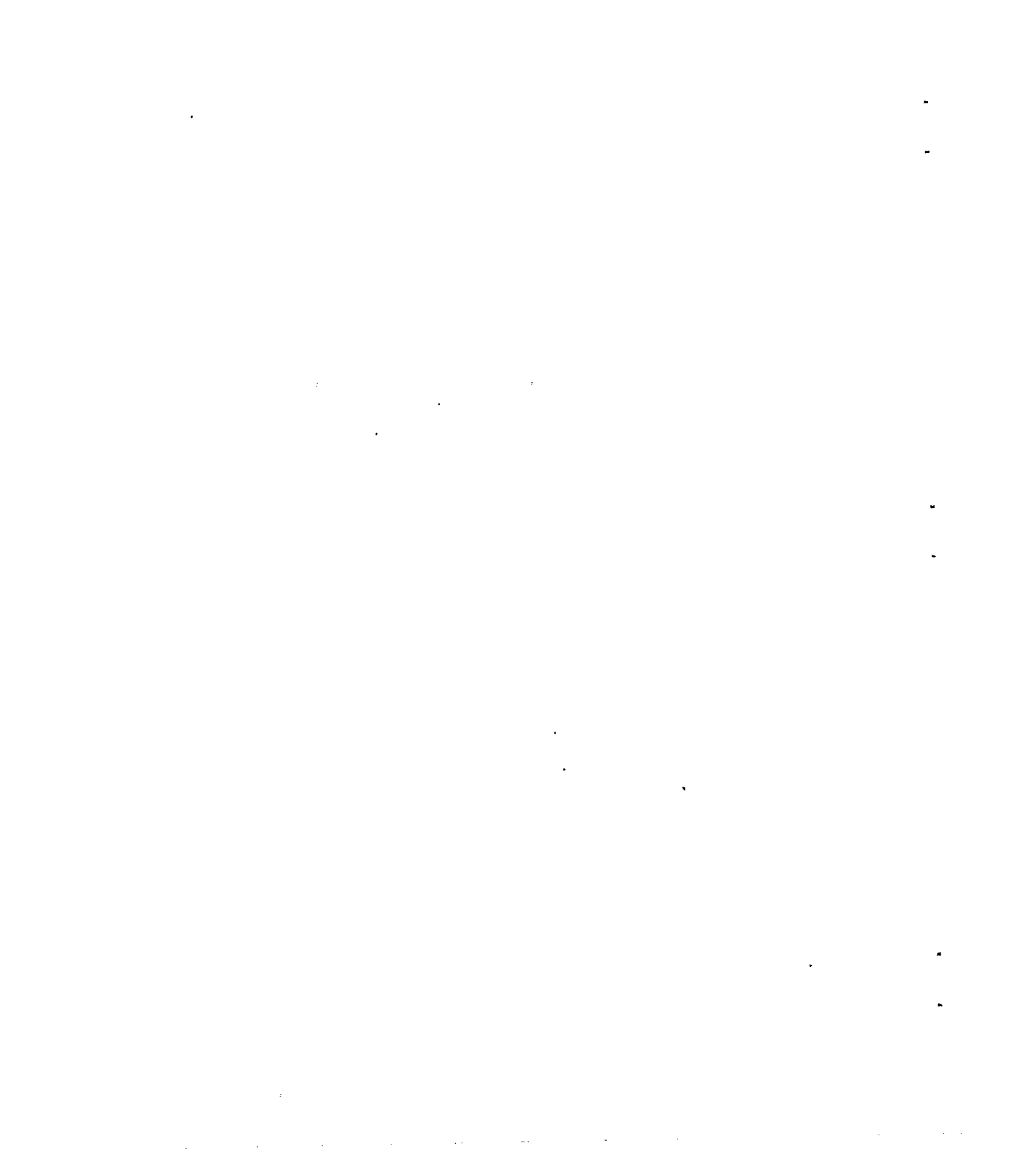


Figure 3.-. Photograph of NACA 3-(3)(05)-05 propeller blade.



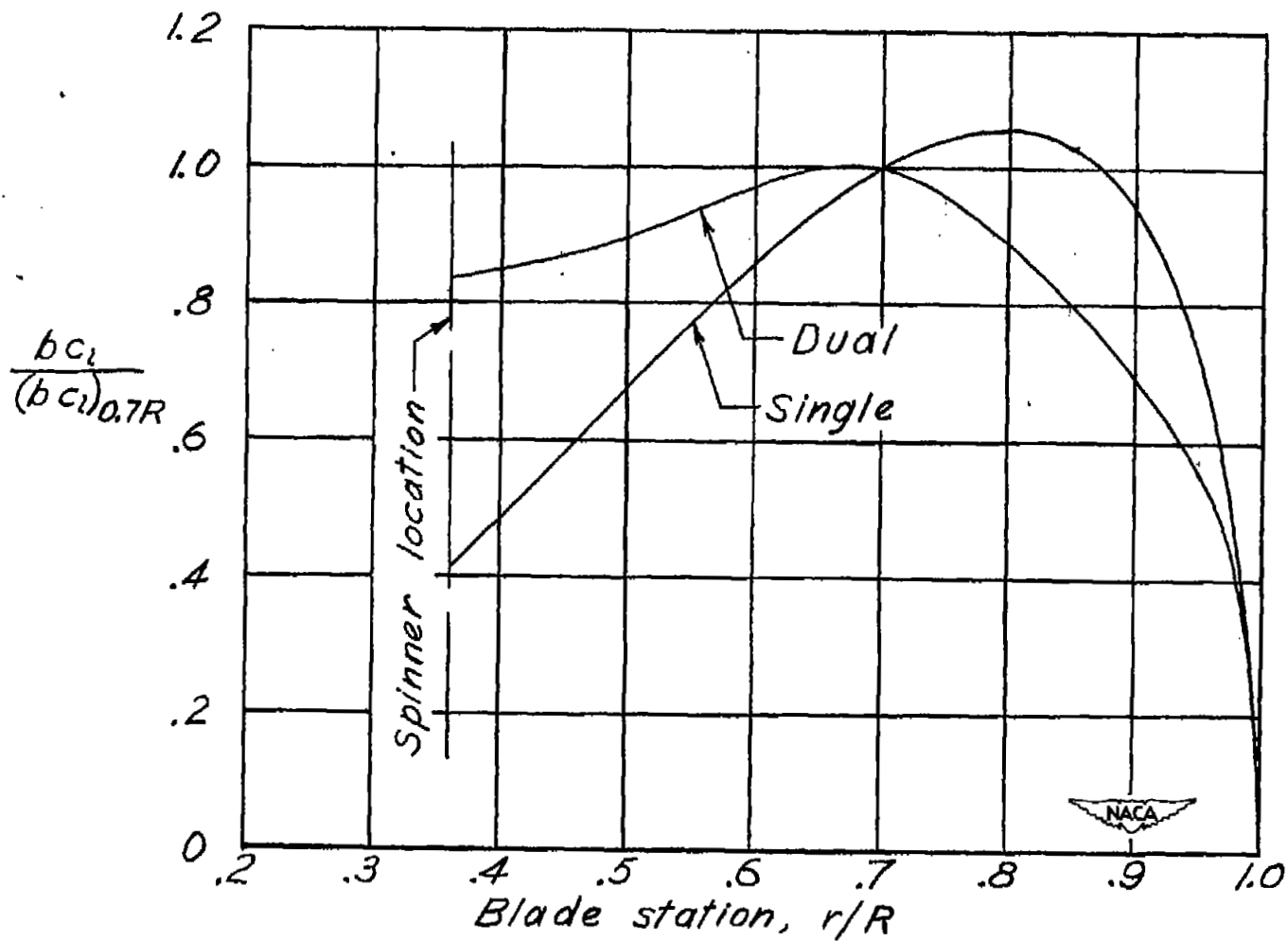


Figure 4.- Comparison of design blade-loading of NACA 3-(3)(05)-05 dual propeller with blade-loading of optimum single-rotating propeller.

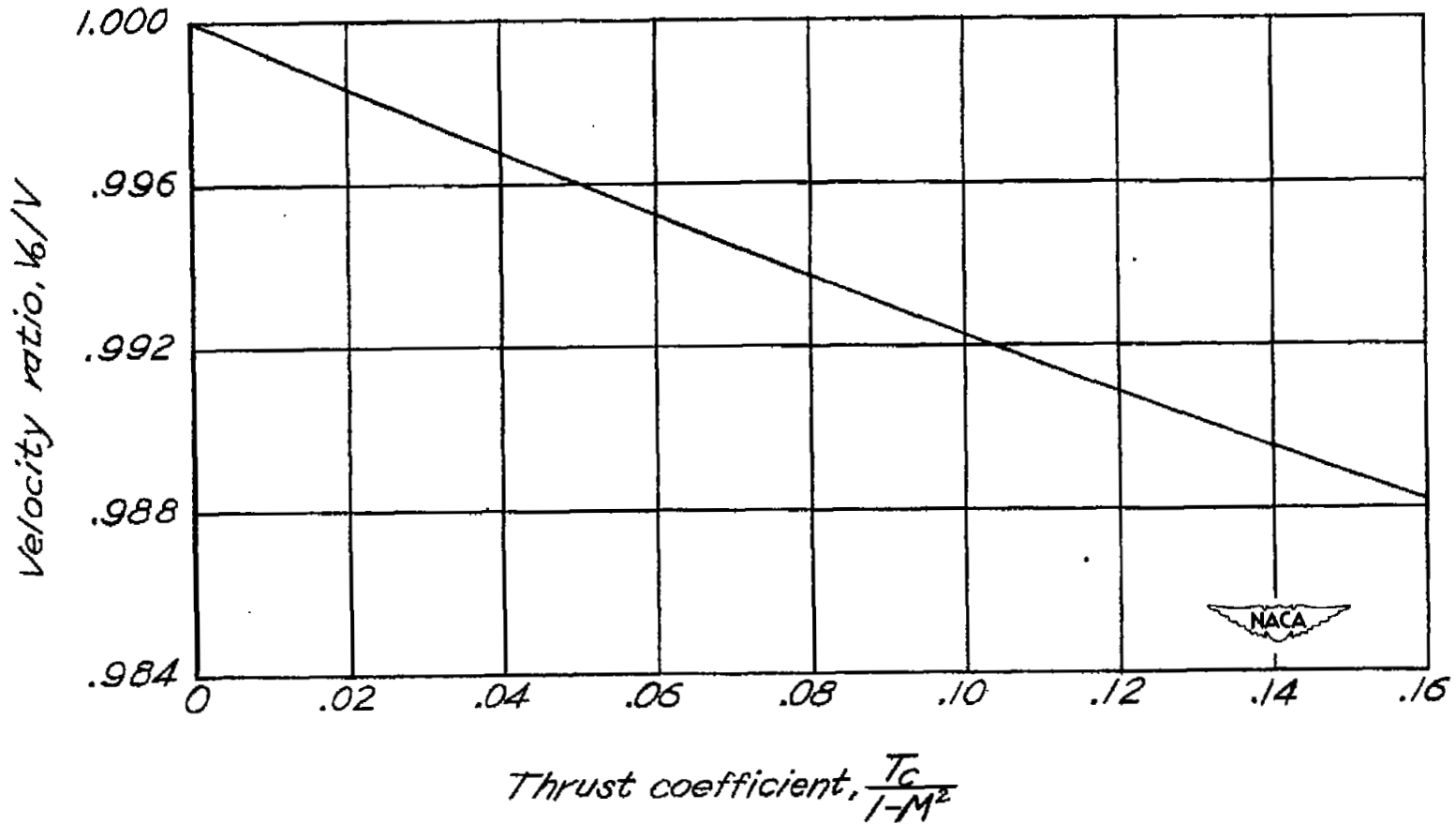
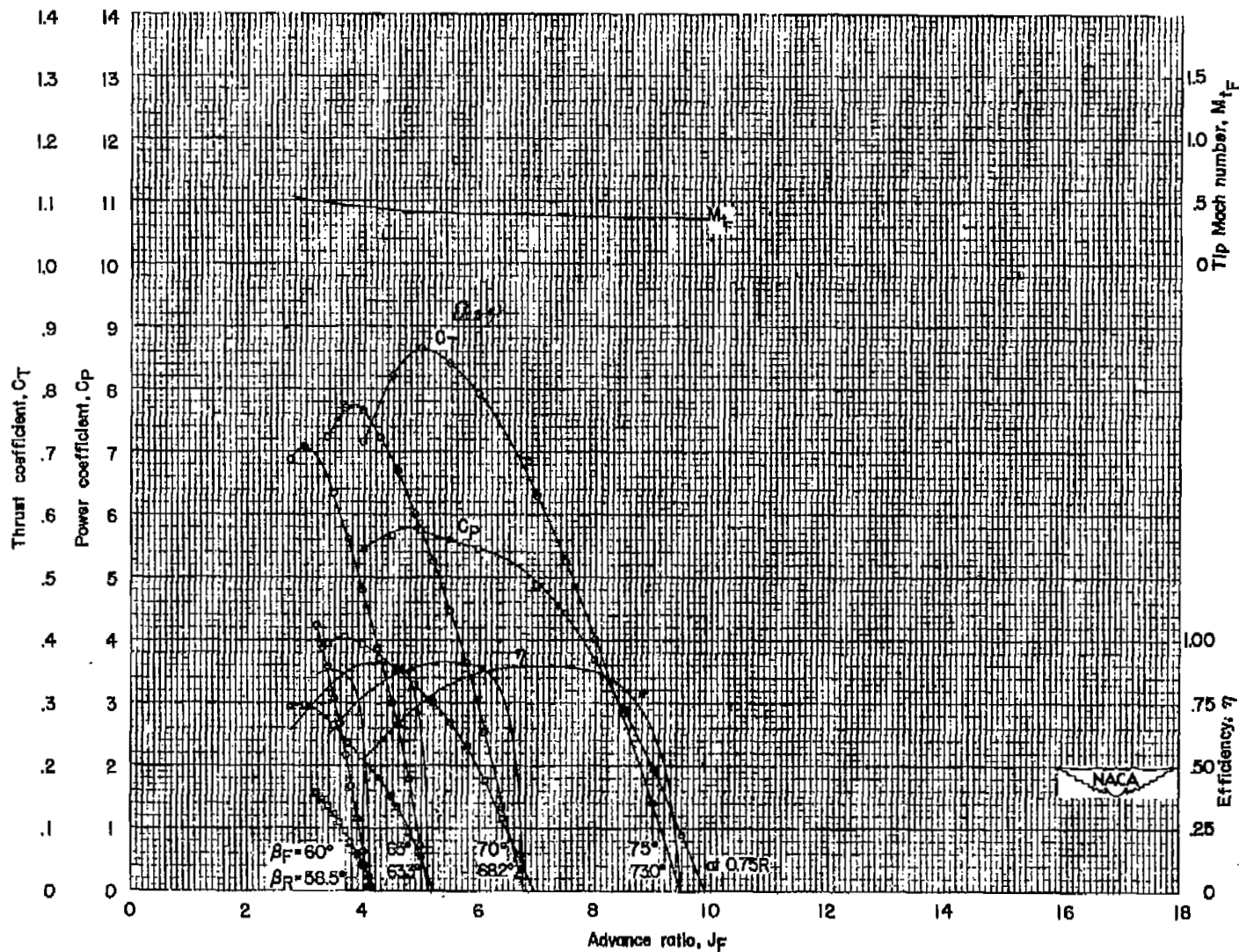
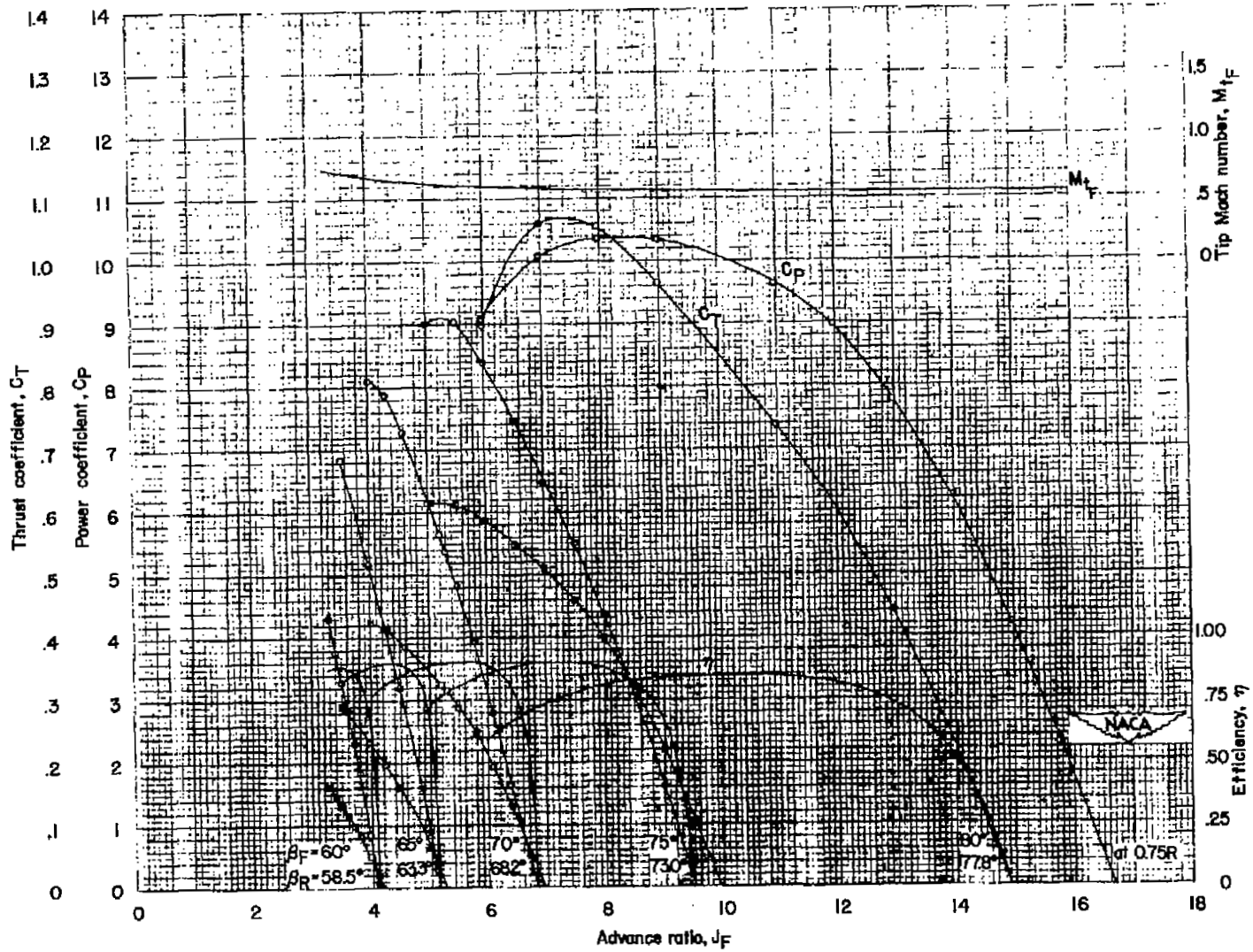


Figure 5.- Tunnel-wall-interference correction for 3-foot-diameter propeller in Langley 8-foot high-speed tunnel.



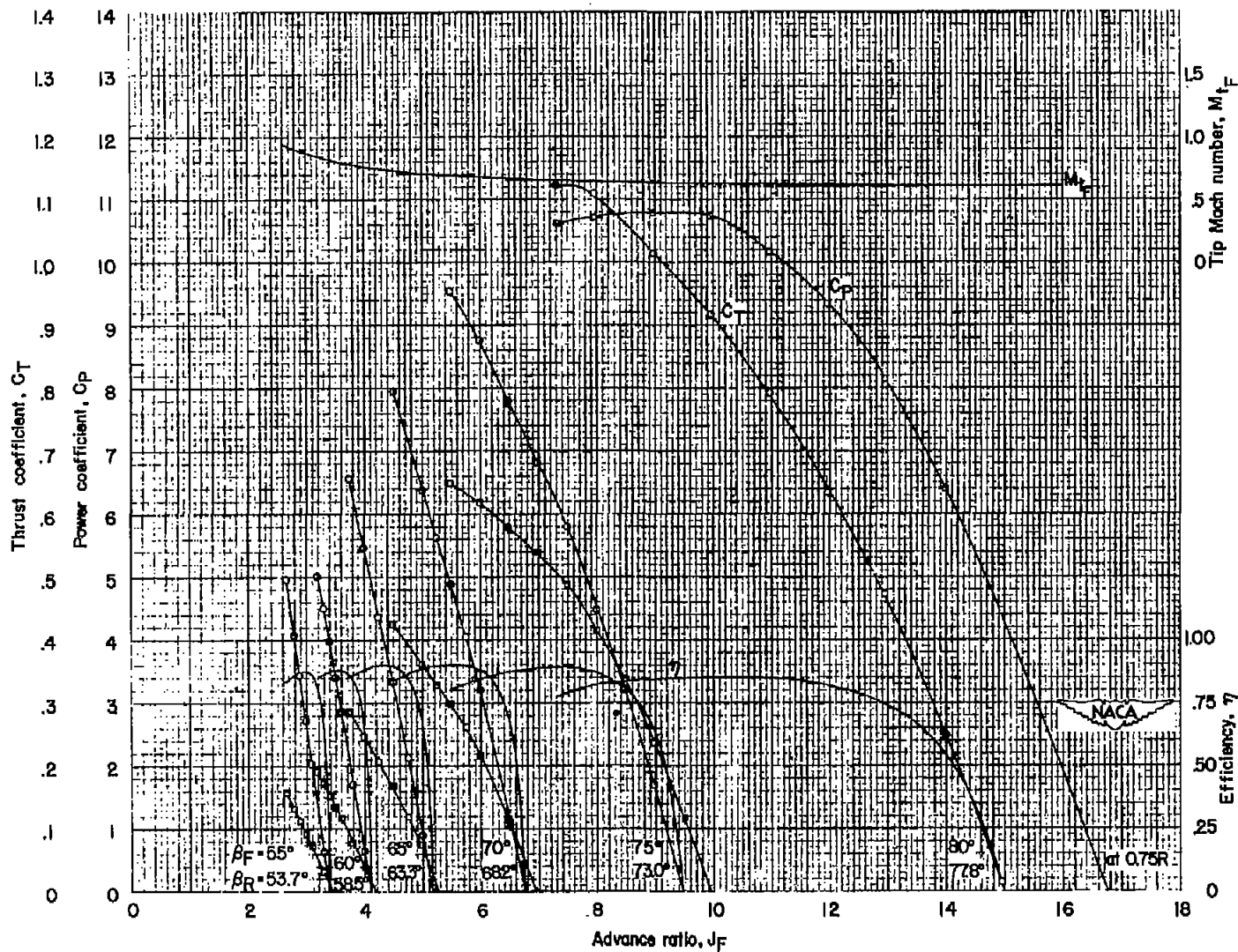
(a) $M = 0.35$.

Figure 6.- Characteristics of NACA 3-(3)(05)-05 eight-blade dual-rotating propeller.



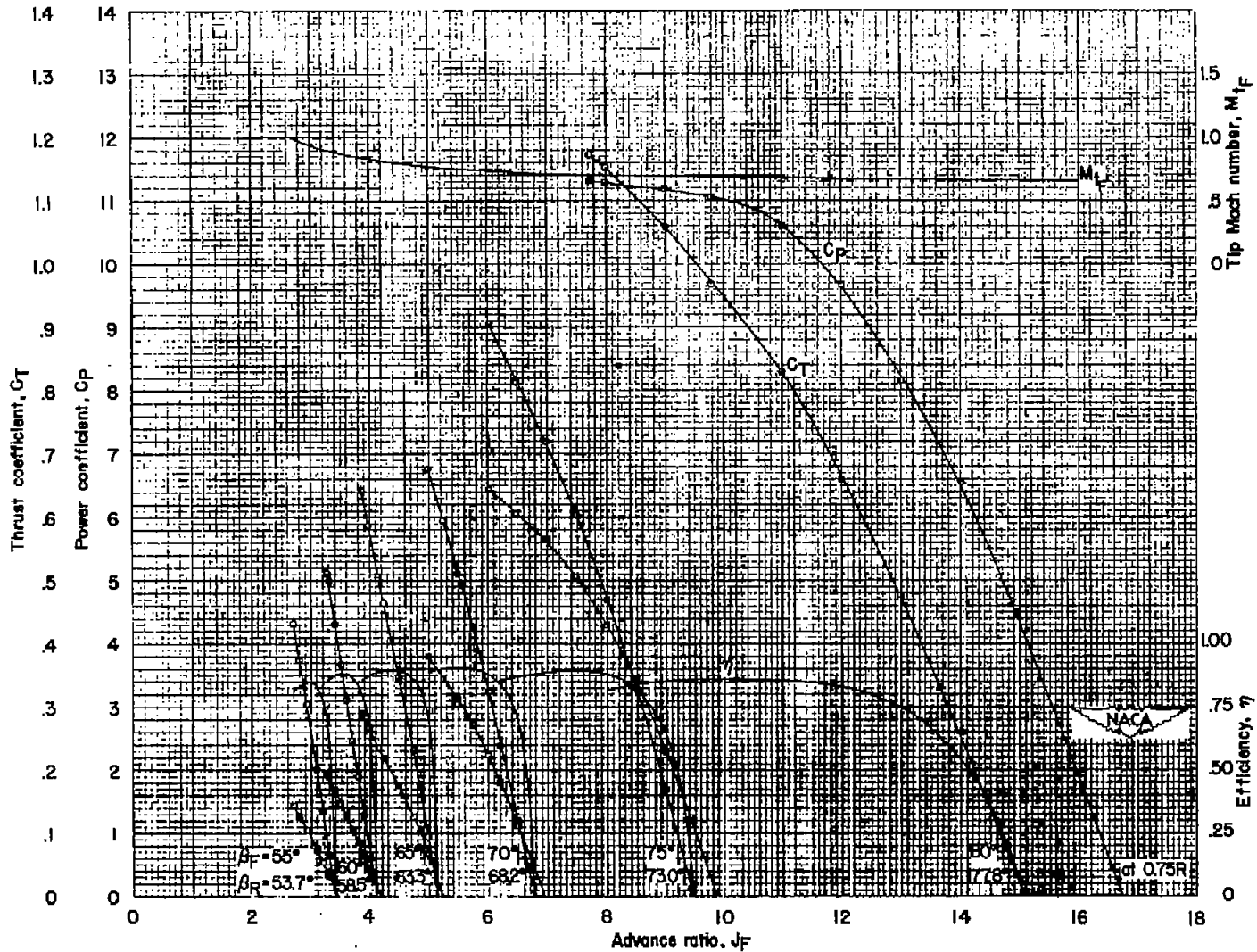
(b) $M = 0.53$.

Figure 6.- Continued.



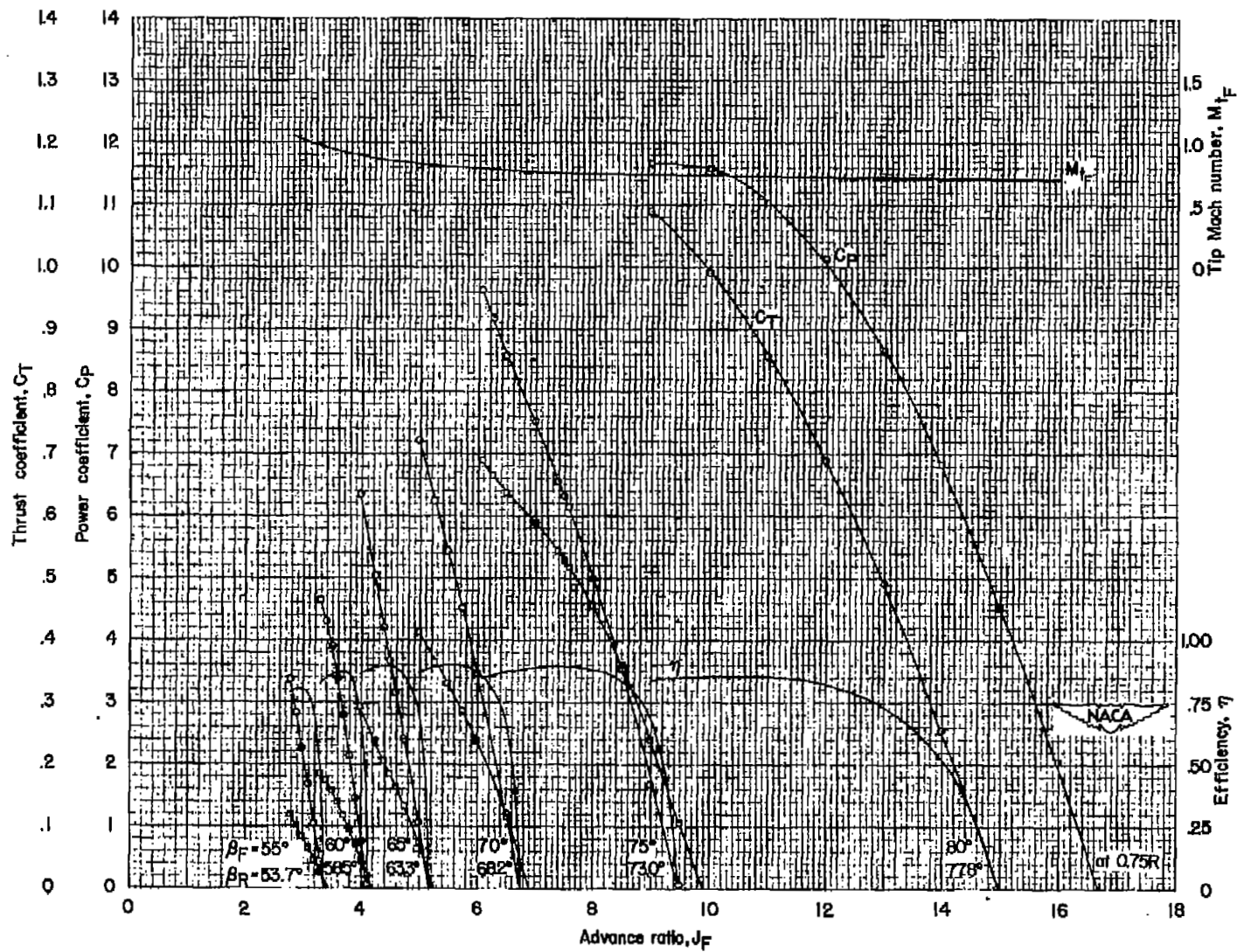
(c) $M = 0.60$.

Figure 6.- Continued.



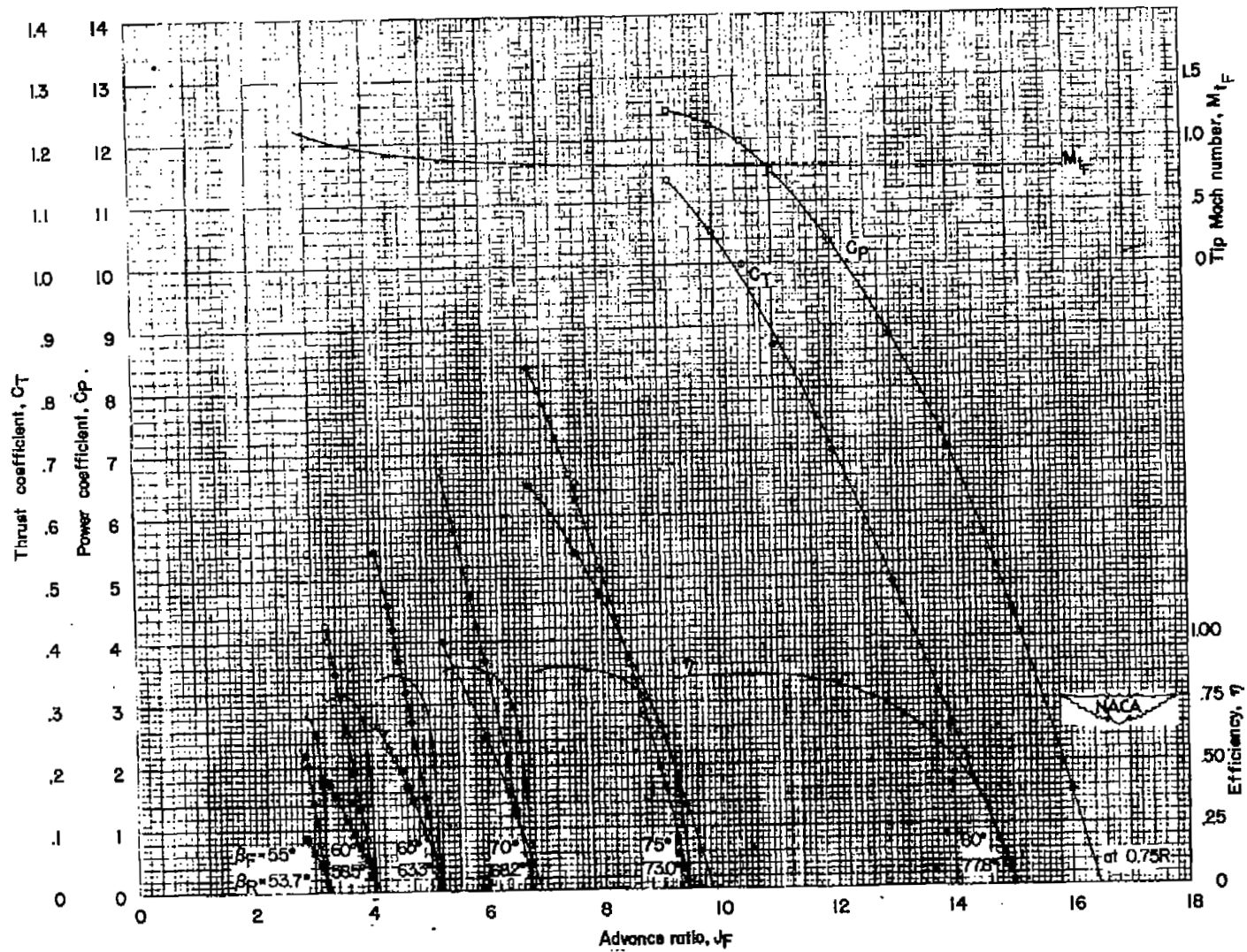
(d) $M = 0.65$.

Figure 6.- Continued.



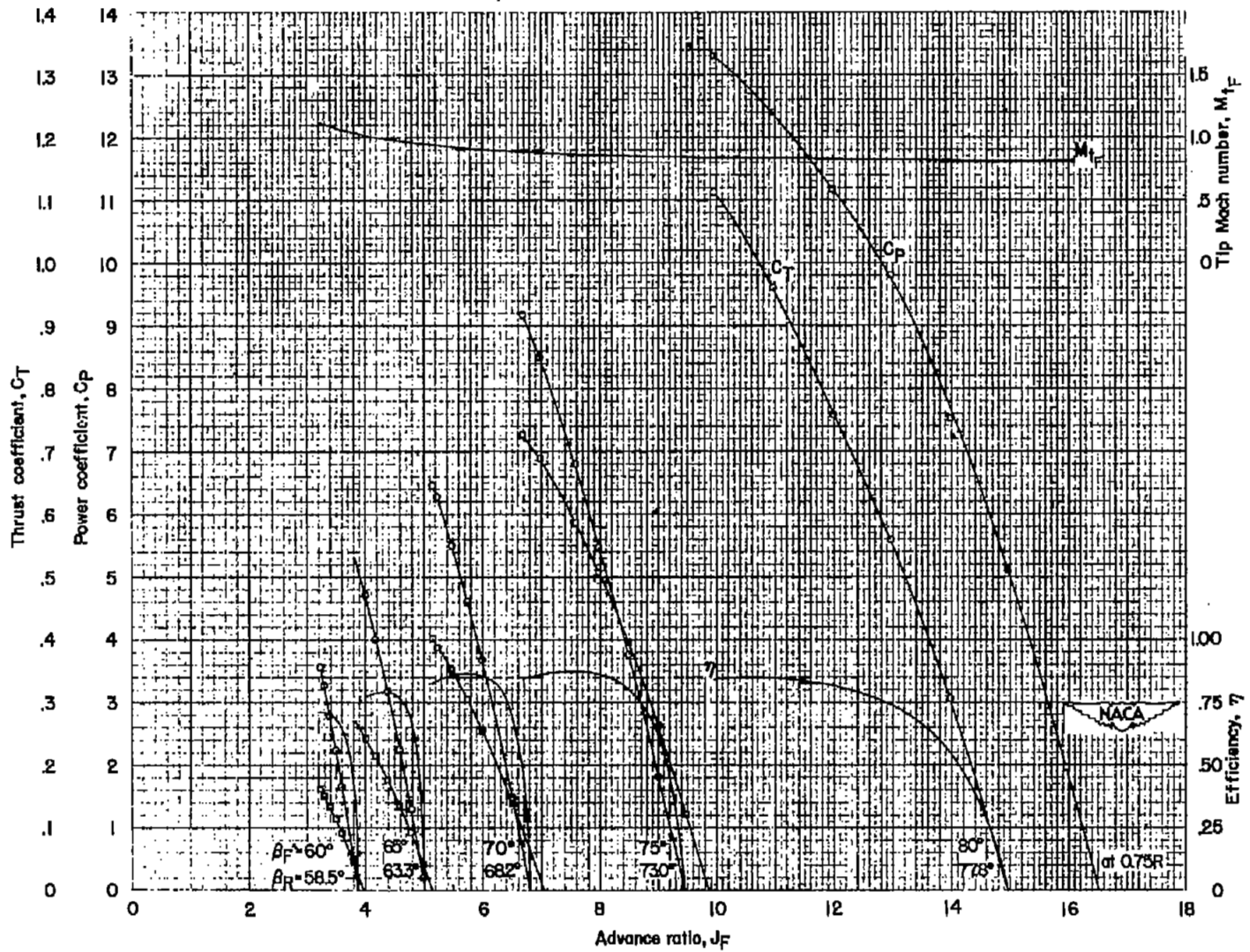
(e) $M = 0.70$.

Figure 6.- Continued.



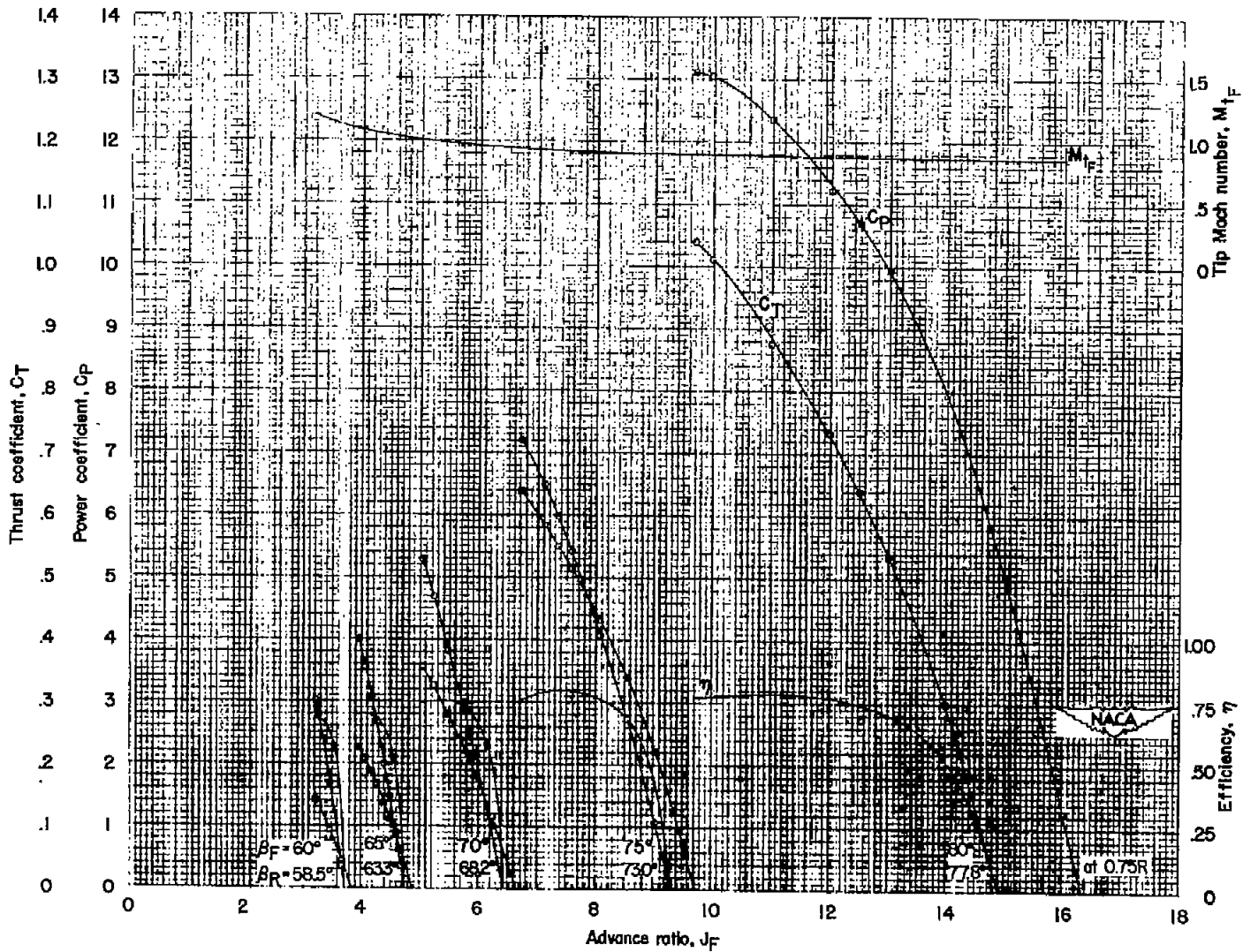
(f) $M = 0.75$.

Figure 6.- Continued.



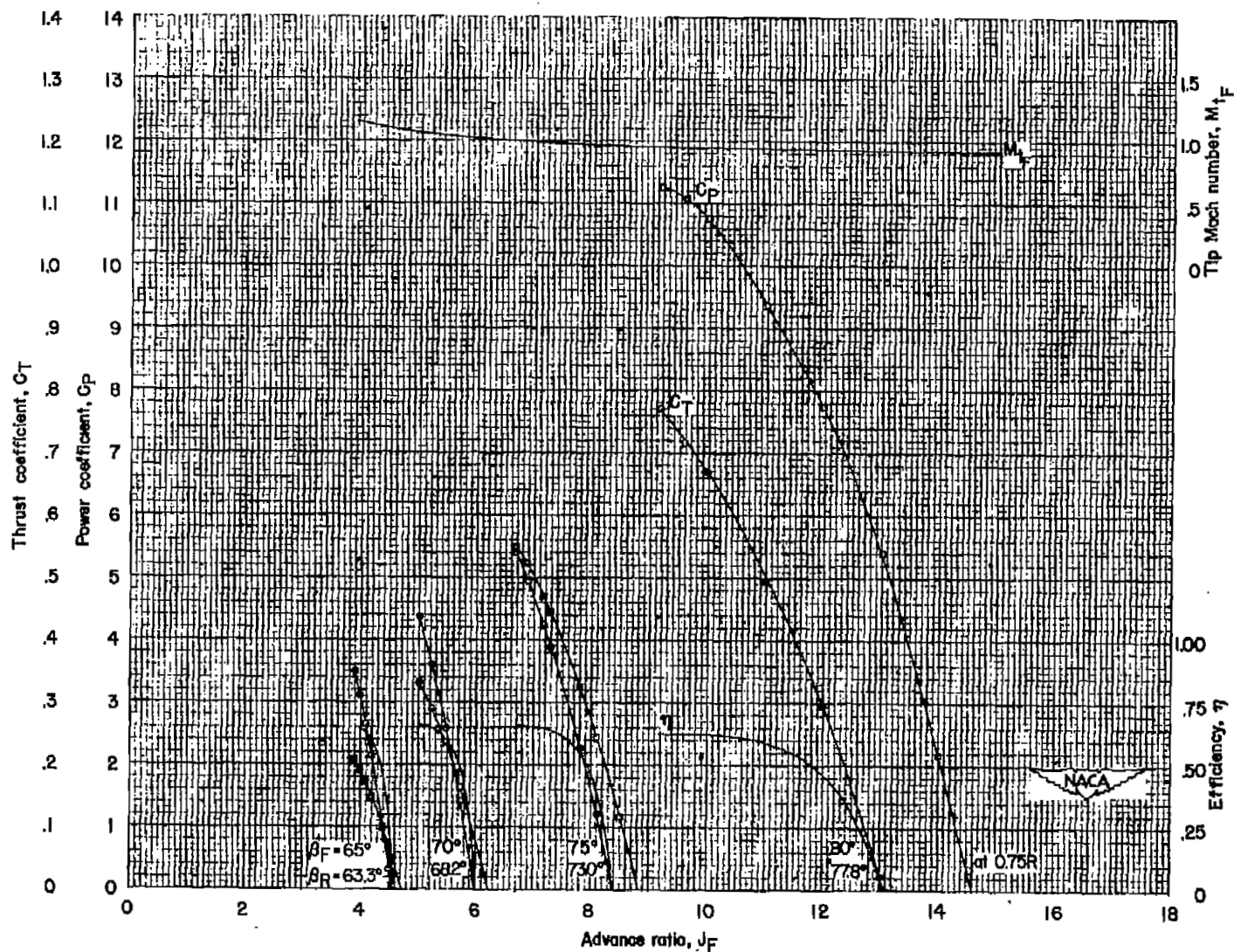
(g) $M = 0.80$.

Figure 6.- Continued.



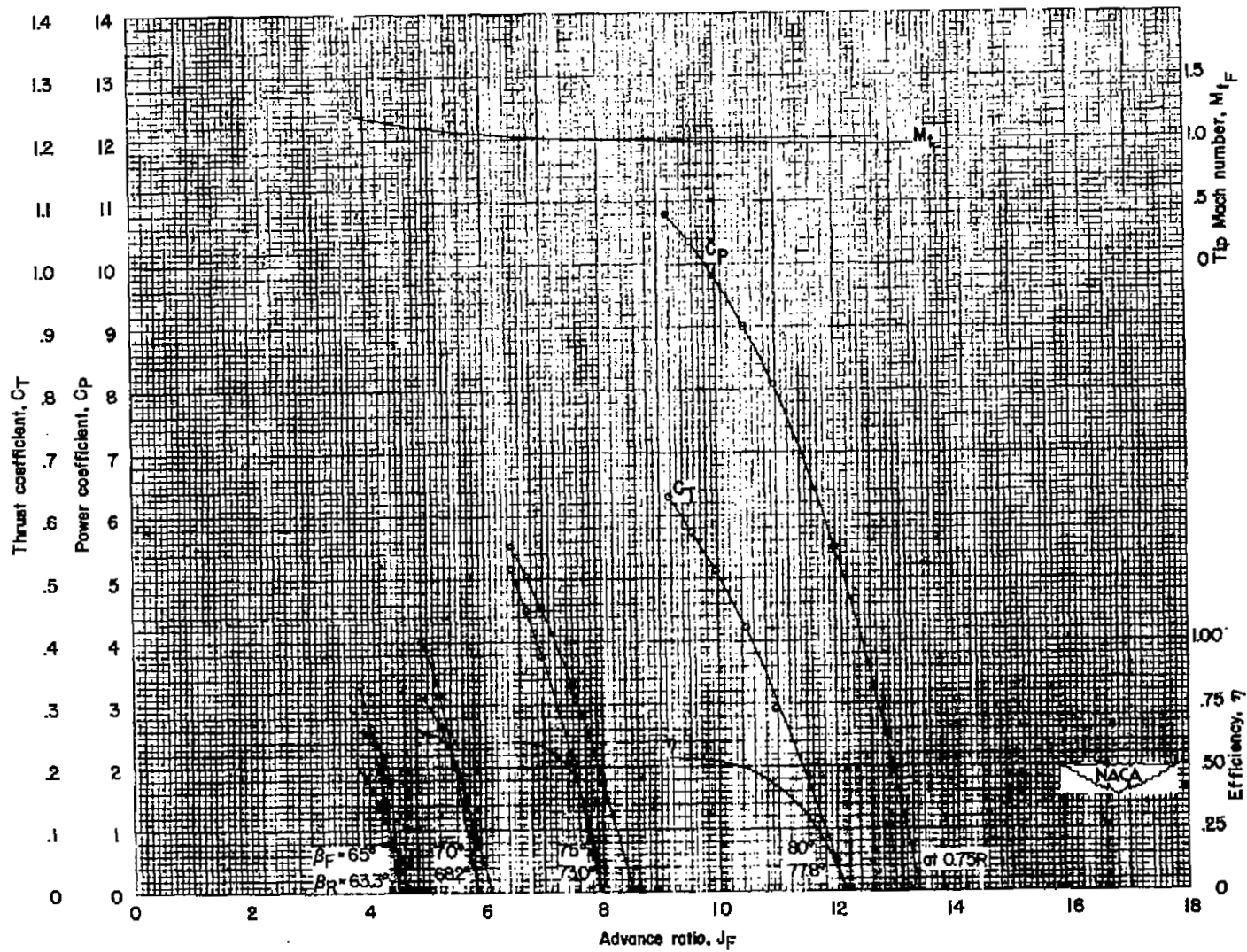
(h) $M = 0.85$.

Figure 6.- Continued.



(i) $M = 0.90$.

Figure 6.- Continued.



(j) $M = 0.925$.

Figure 6.- Concluded.

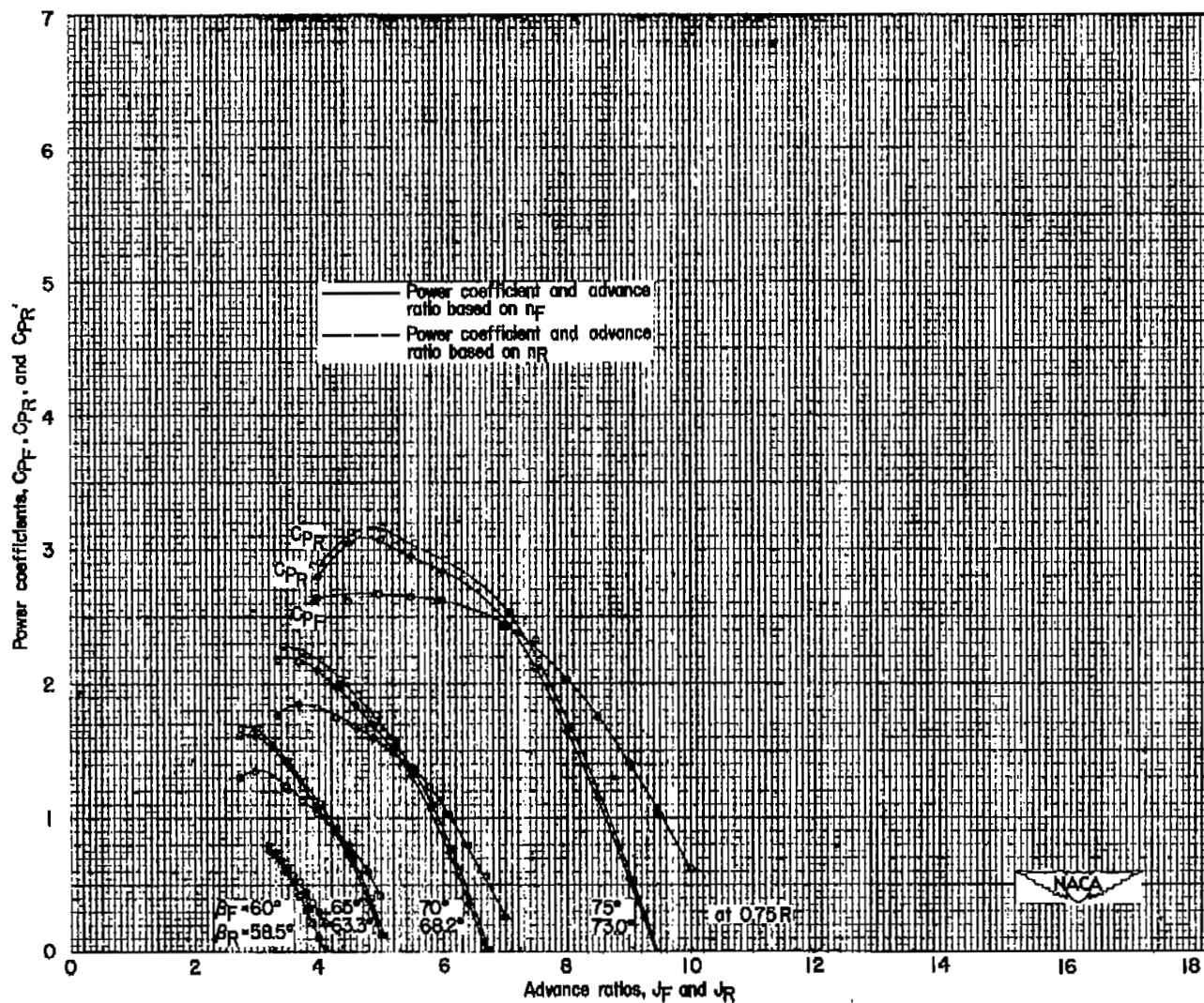
(a) $M = 0.35$.

Figure 7.- Individual power coefficient curves of NACA 3-(3)(05)-05 eight-blade dual-rotating propeller.

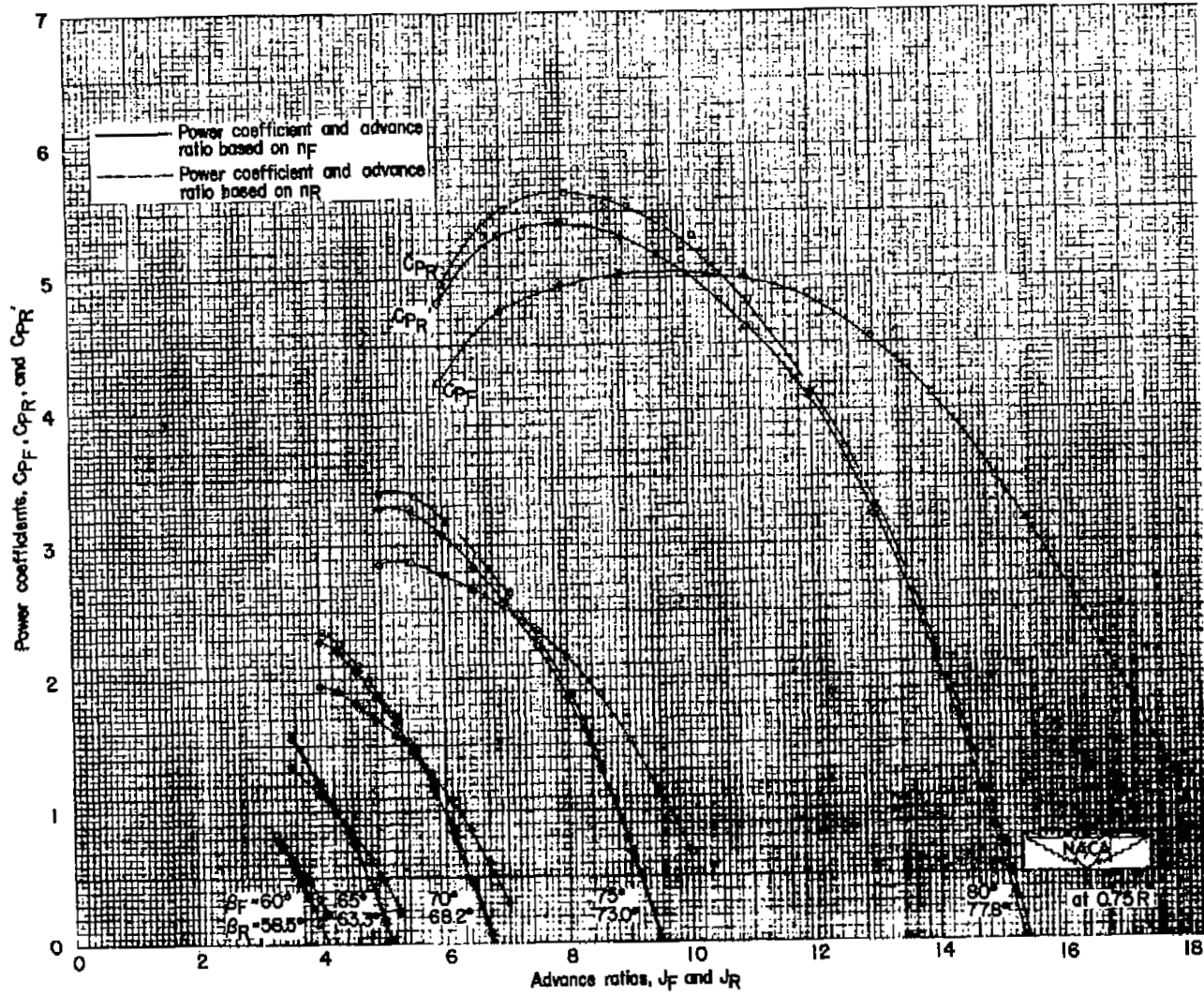
(b) $M = 0.53$.

Figure 7.- Continued.

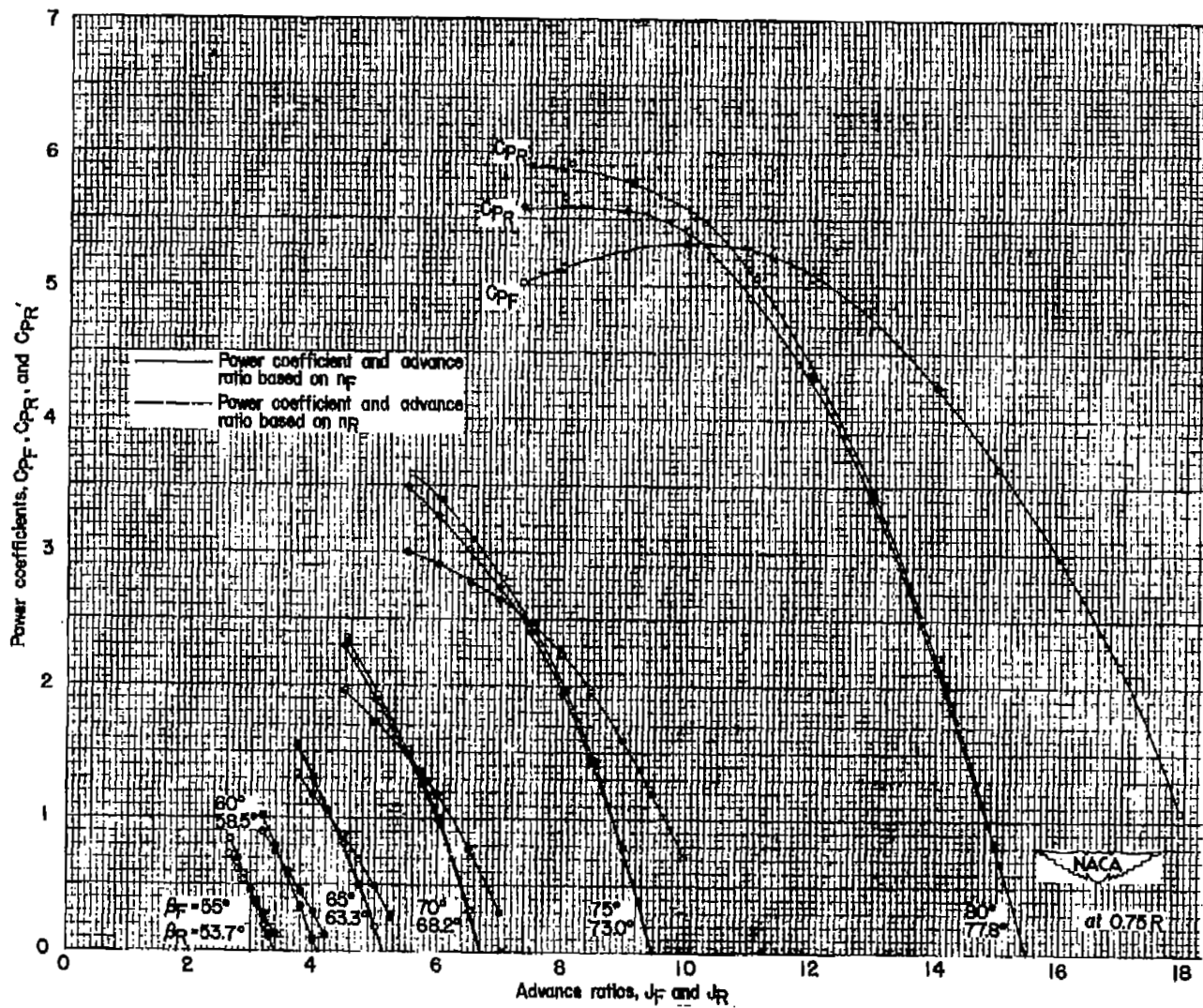
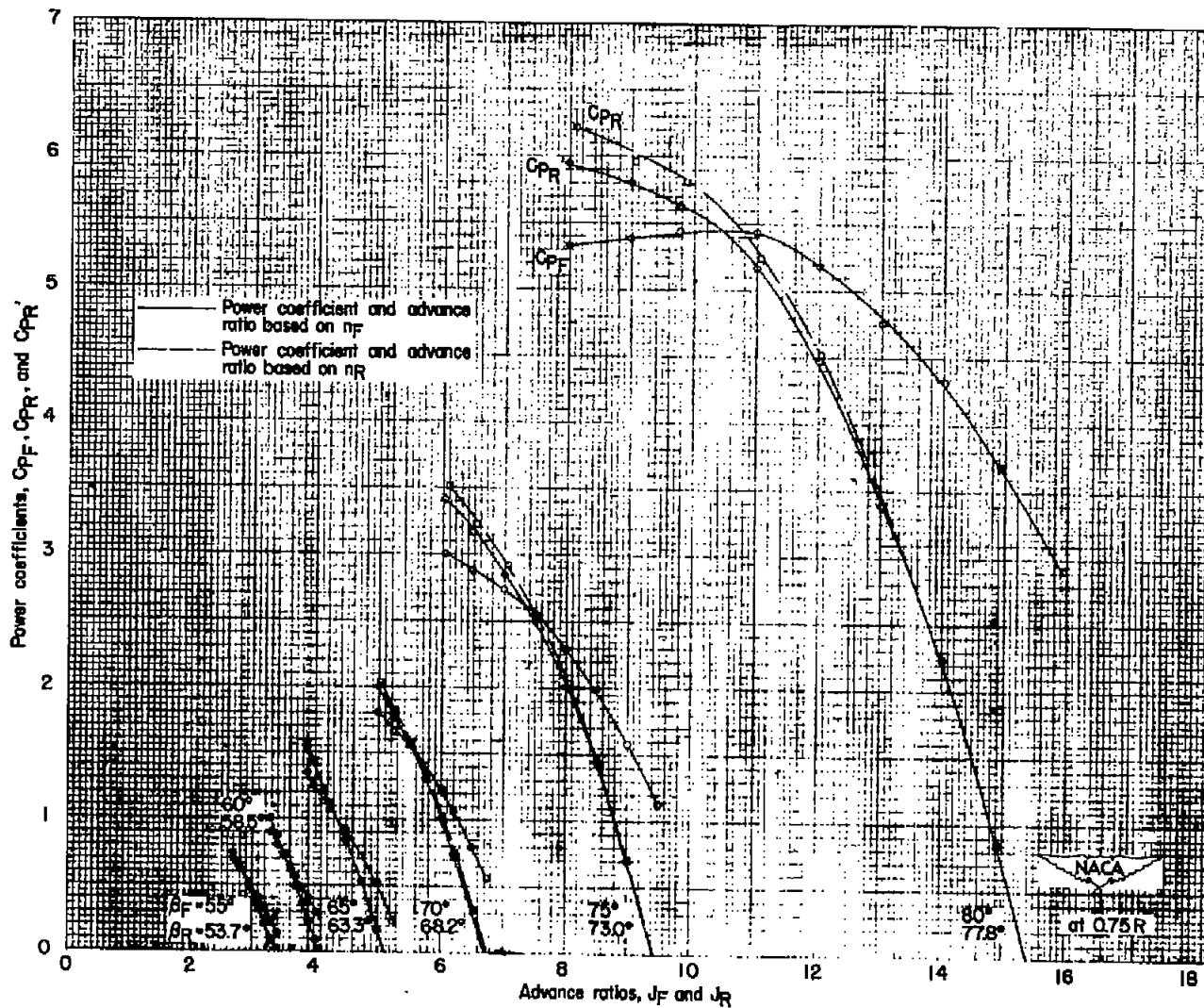
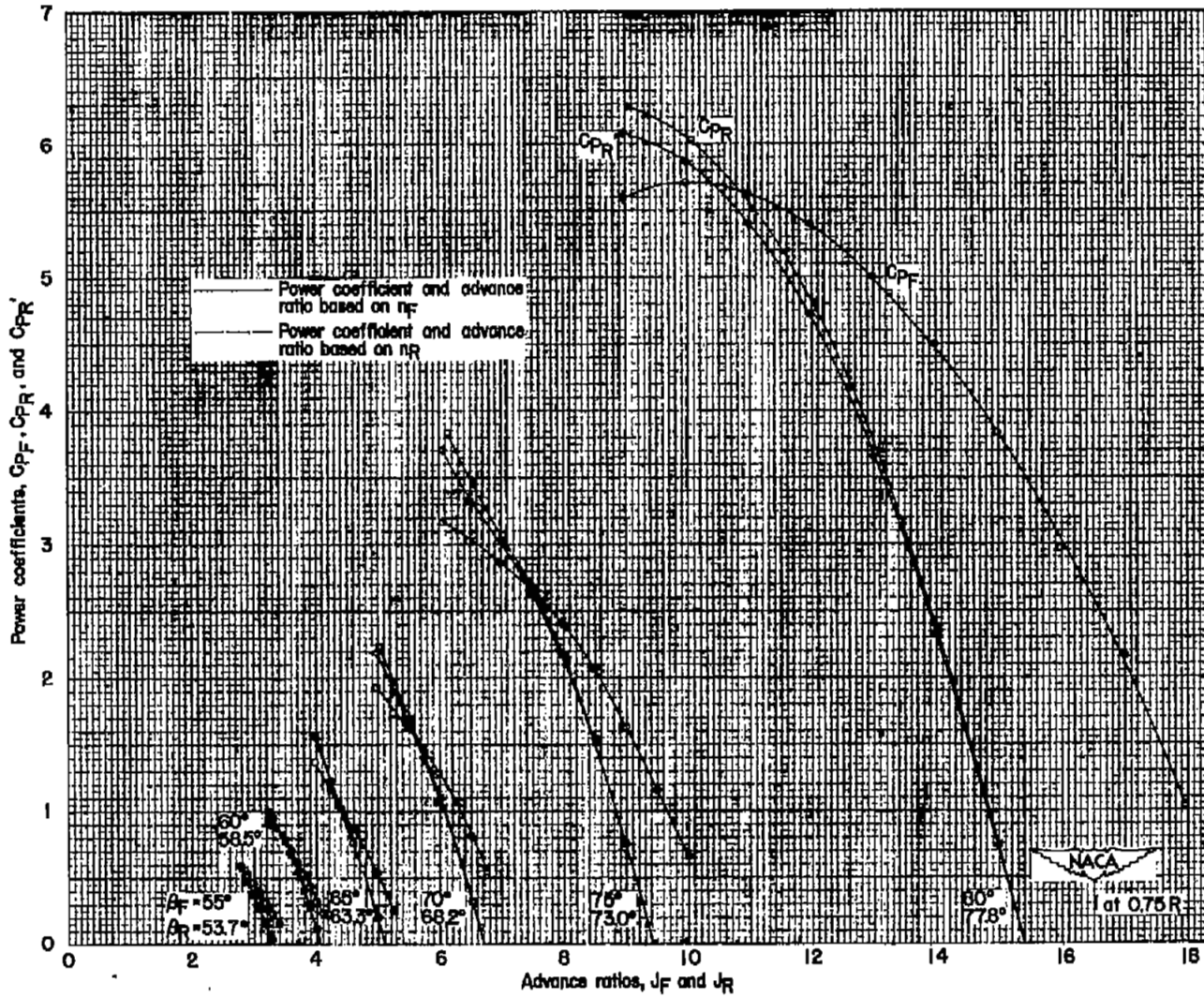
(c) $M = 0.60$.

Figure 7.- Continued.



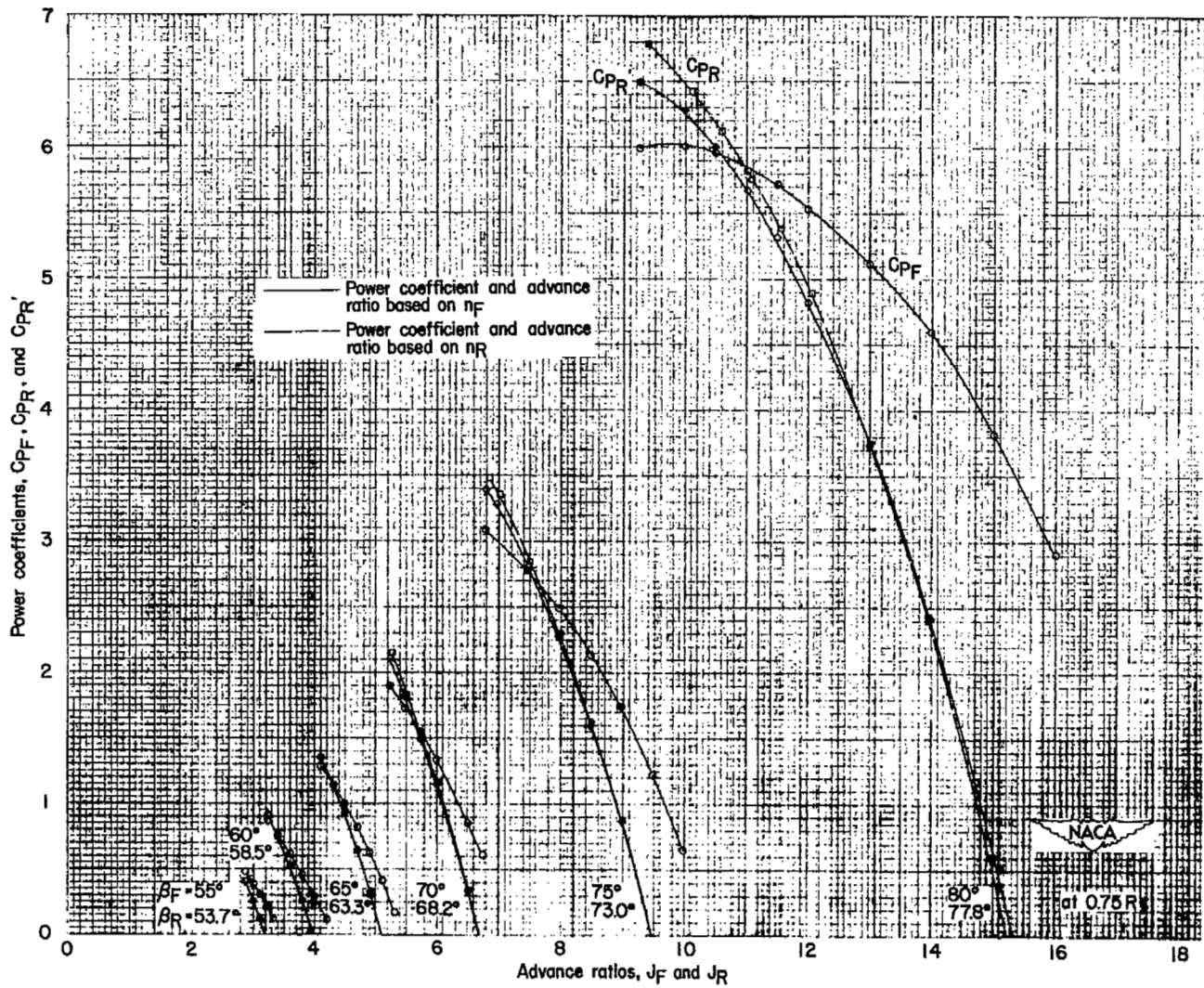
(d) $M = 0.65$.

Figure 7.- Continued.



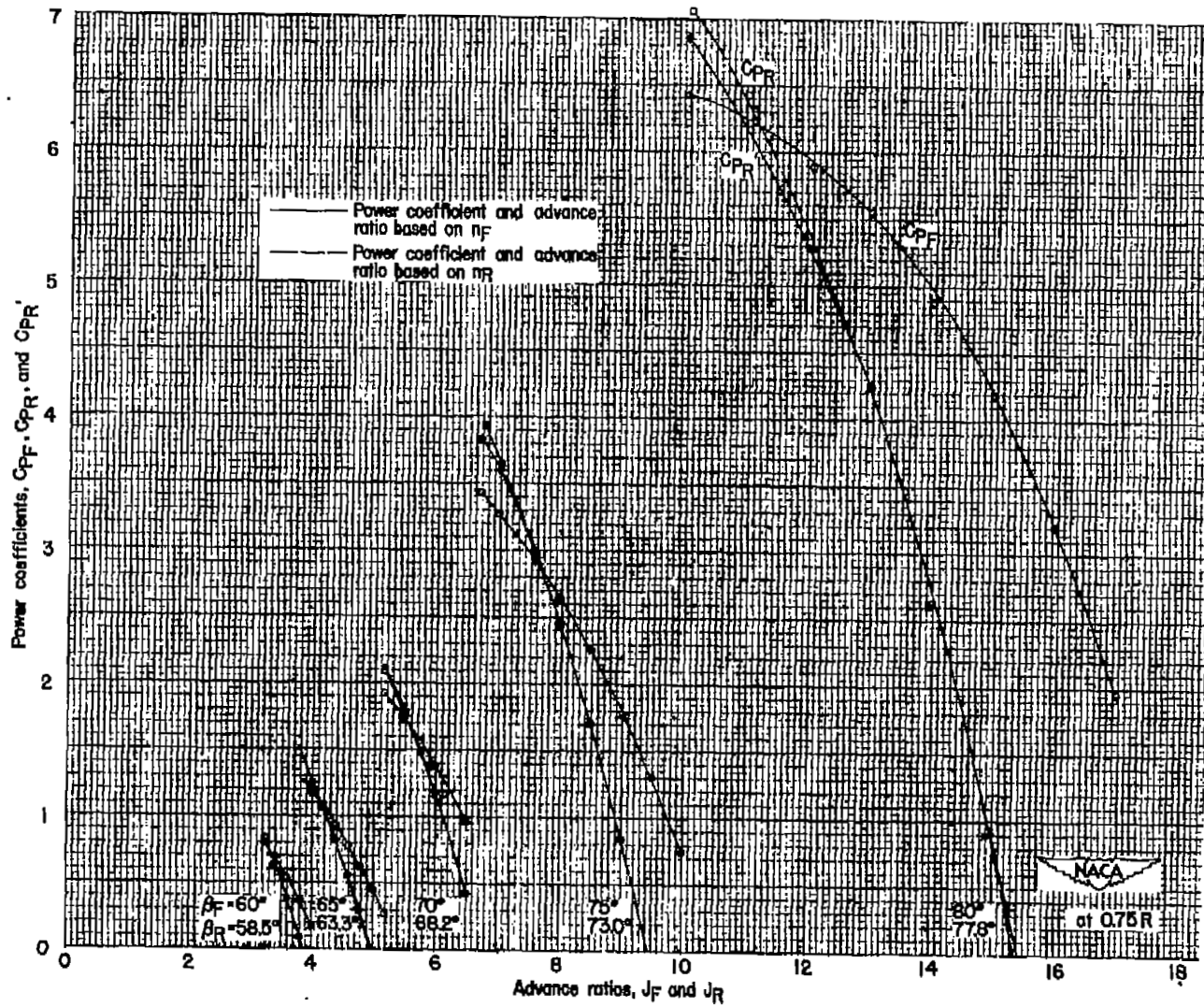
(e) $M = 0.70$.

Figure 7.- Continued.



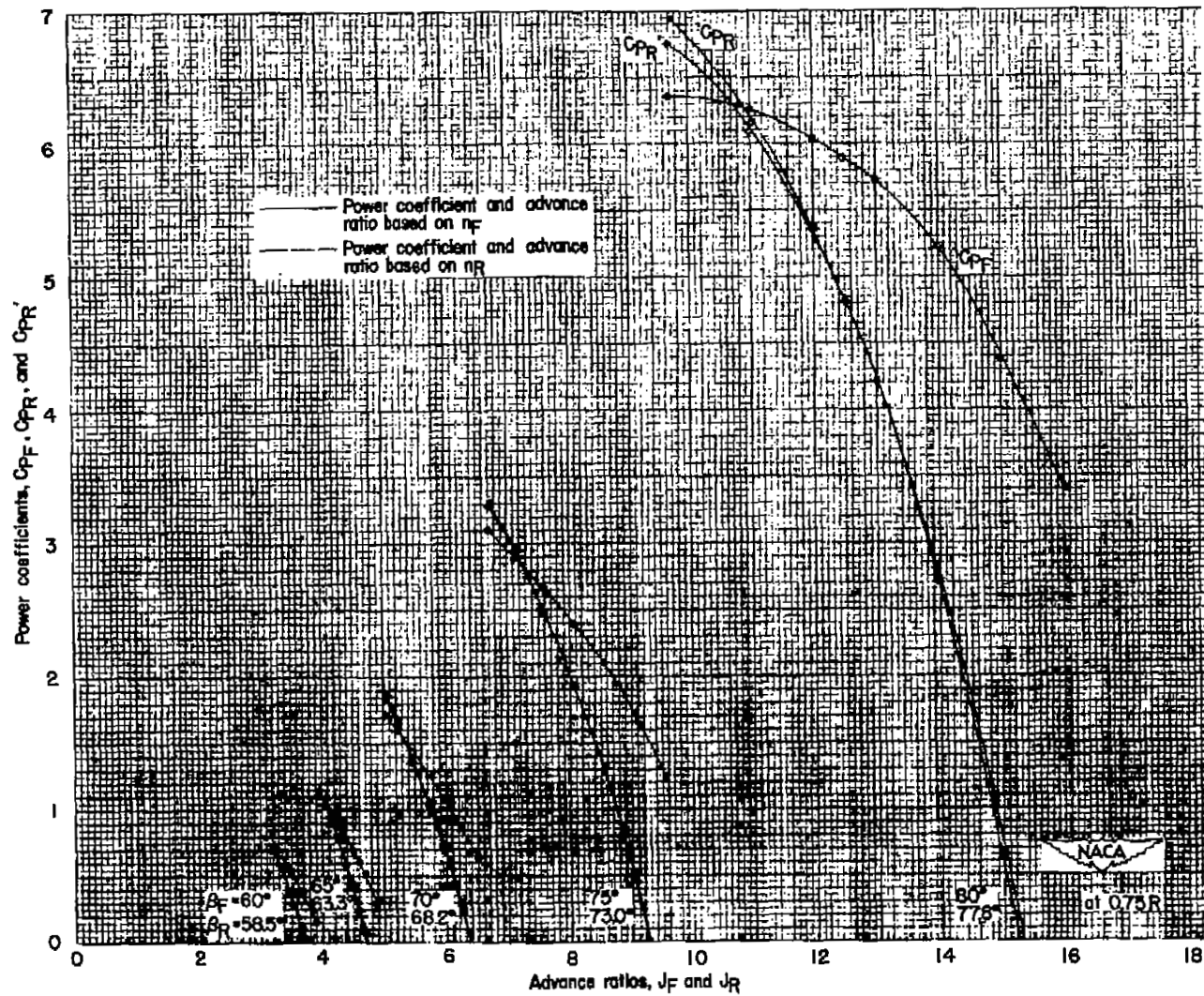
(f) $M = 0.75$.

Figure 7.- Continued.



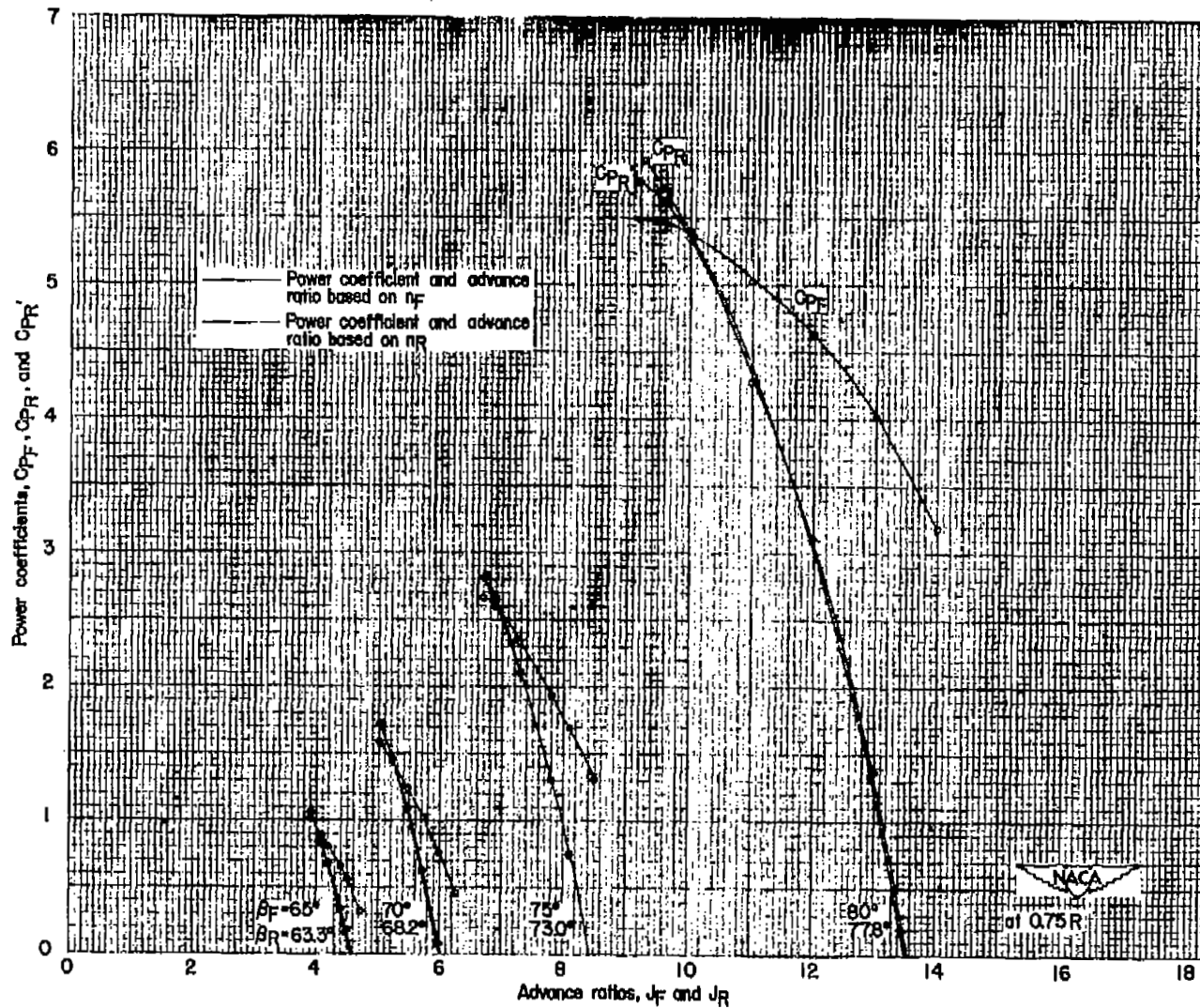
(g) $M = 0.80$.

Figure 7.- Continued.



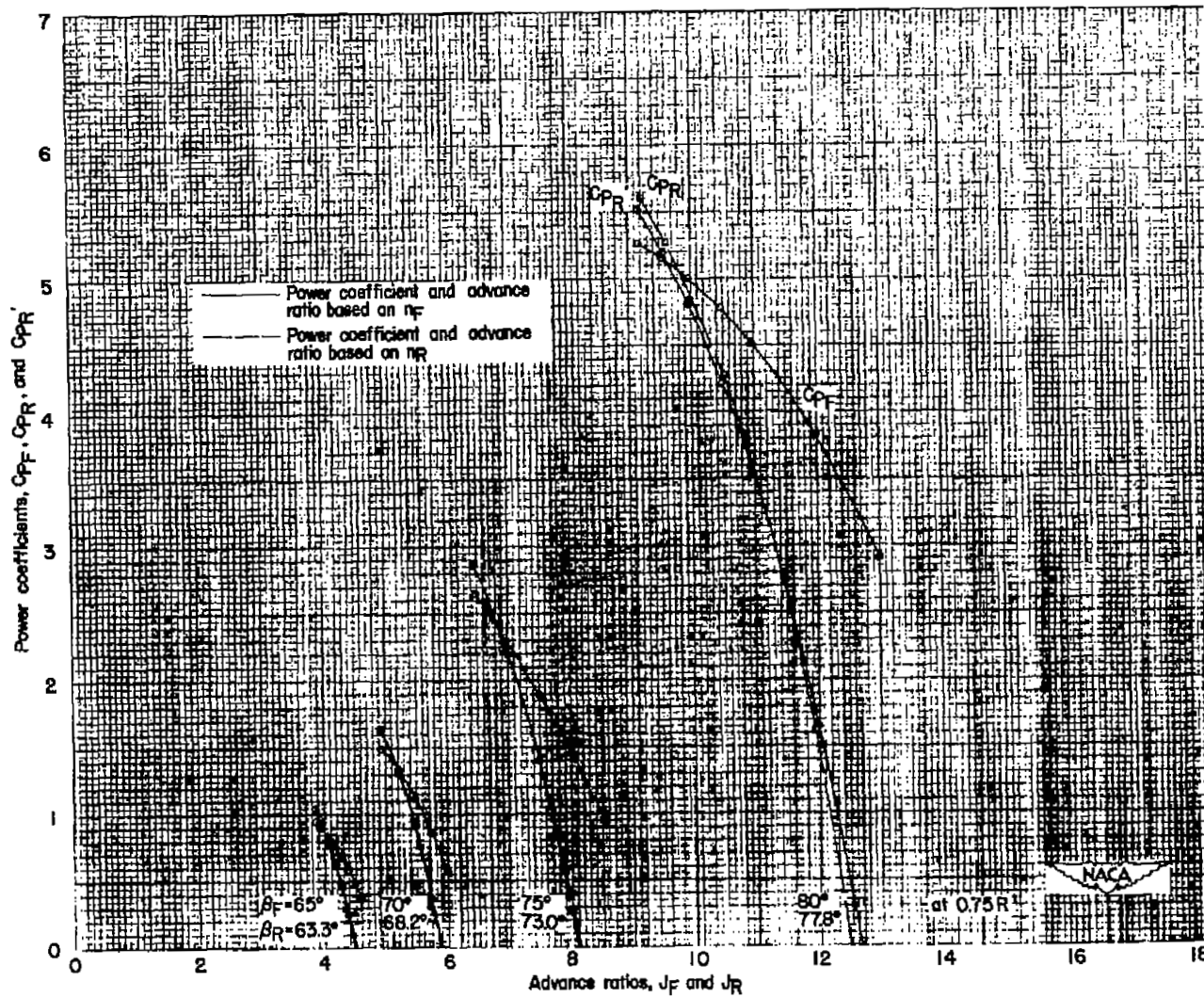
(h) $M = 0.85$.

Figure 7.- Continued.



(1) $M = 0.90$.

Figure 7.- Continued.



(j) $M = 0.925$.

Figure 7.- Concluded.

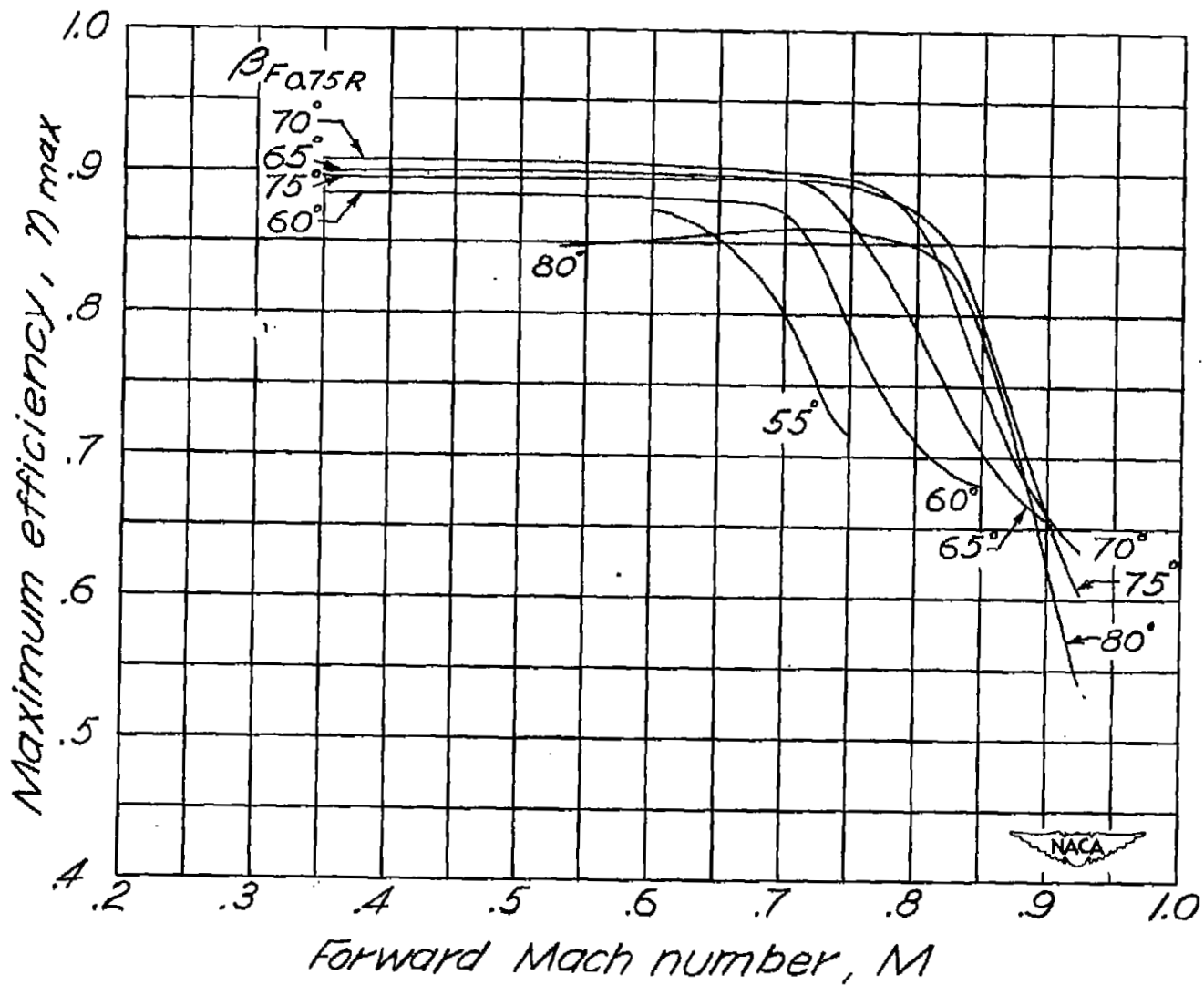


Figure 8.- Variations of maximum efficiency with forward Mach number for NACA 3-(3)(05)-05 eight-blade dual propeller.

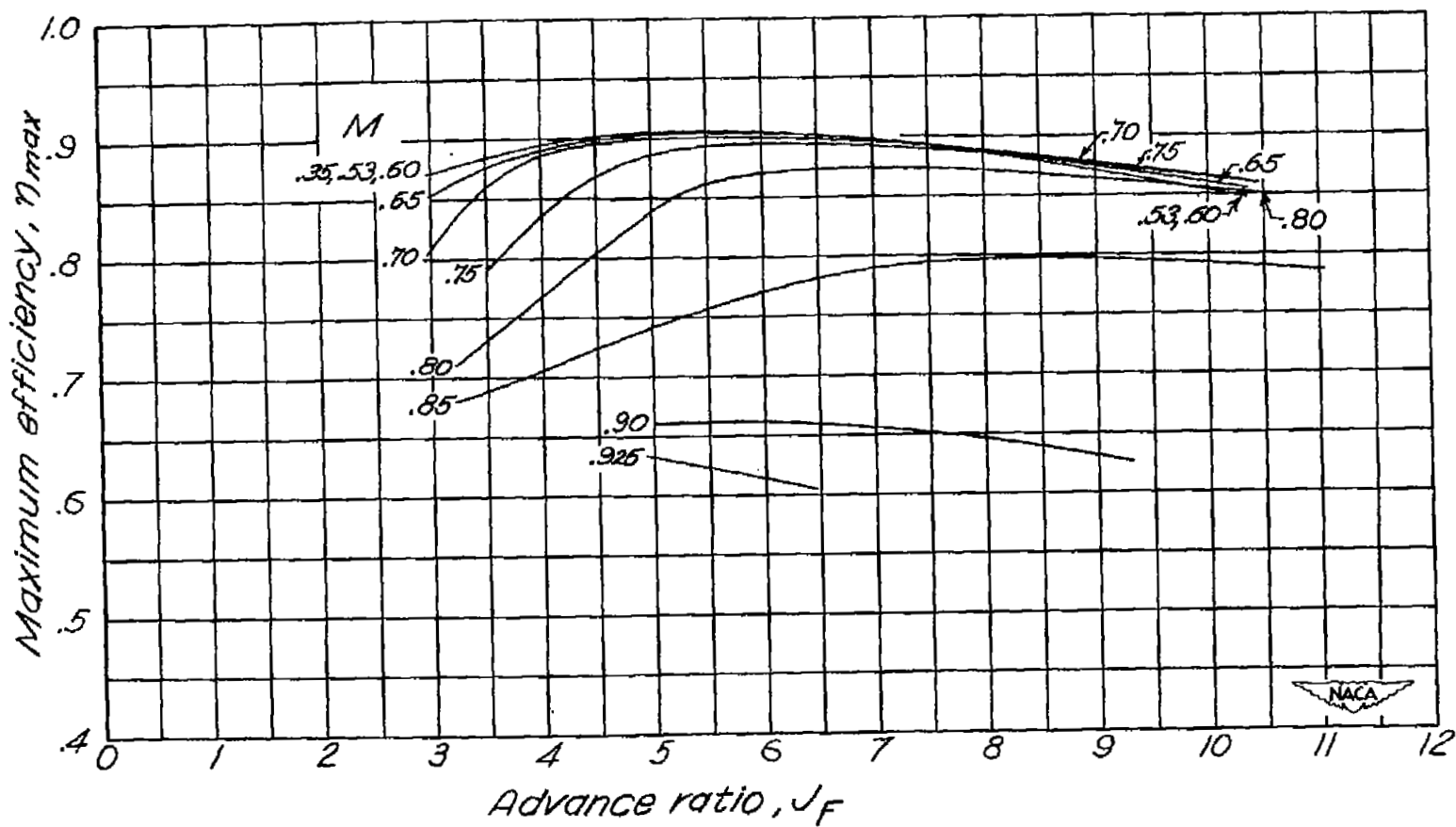
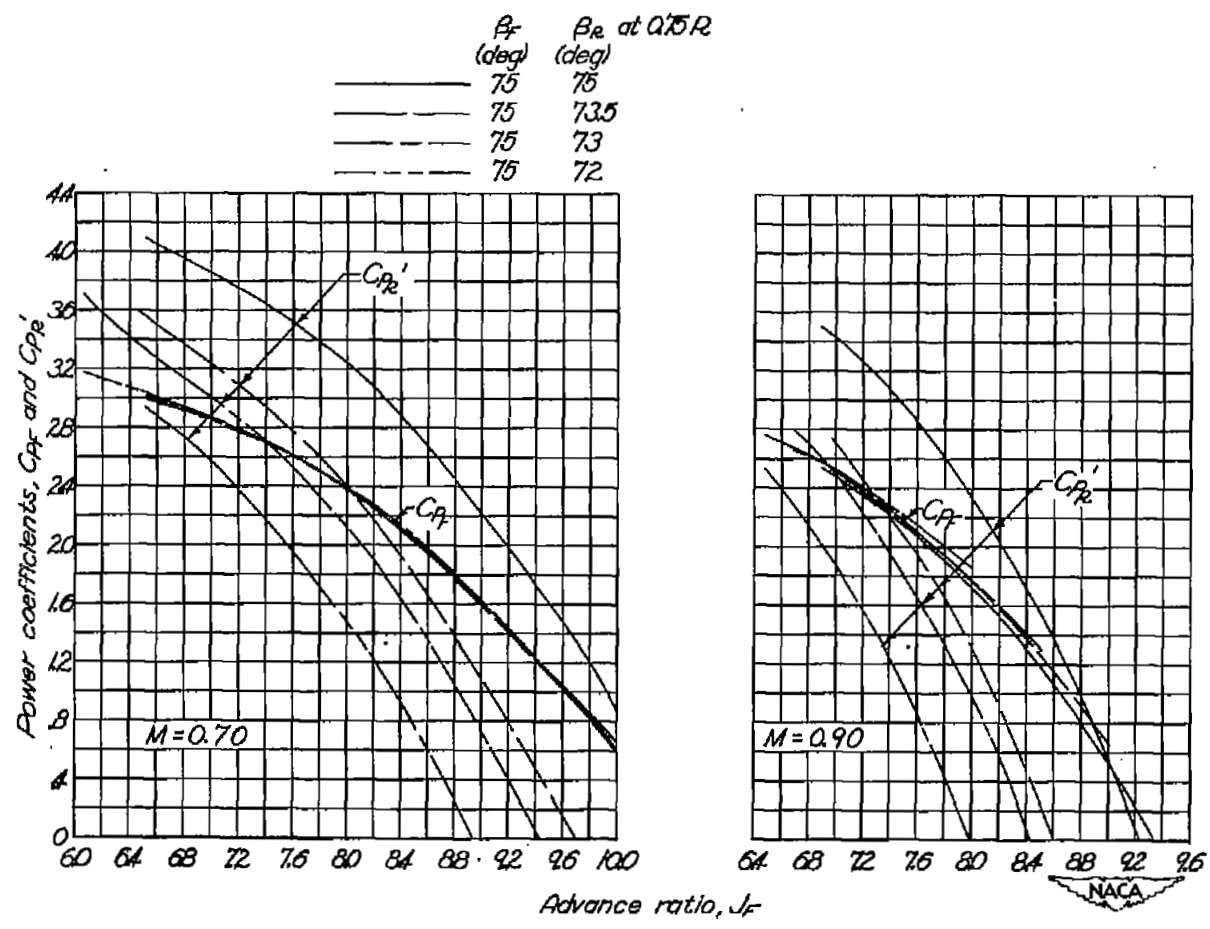
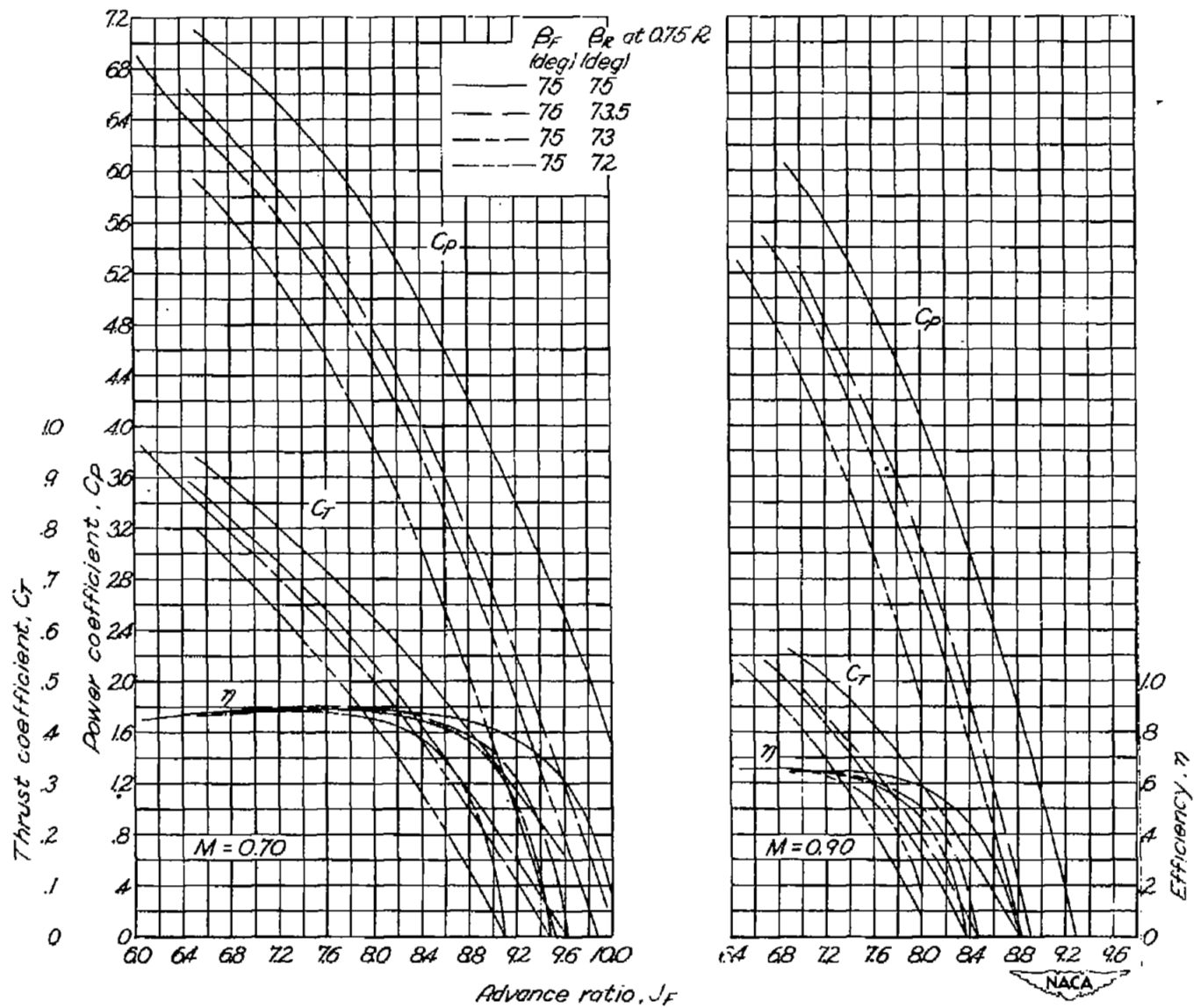


Figure 9.- Variation of maximum efficiency with advance ratio for NACA 3-(3)(05)-05 eight-blade dual propeller.



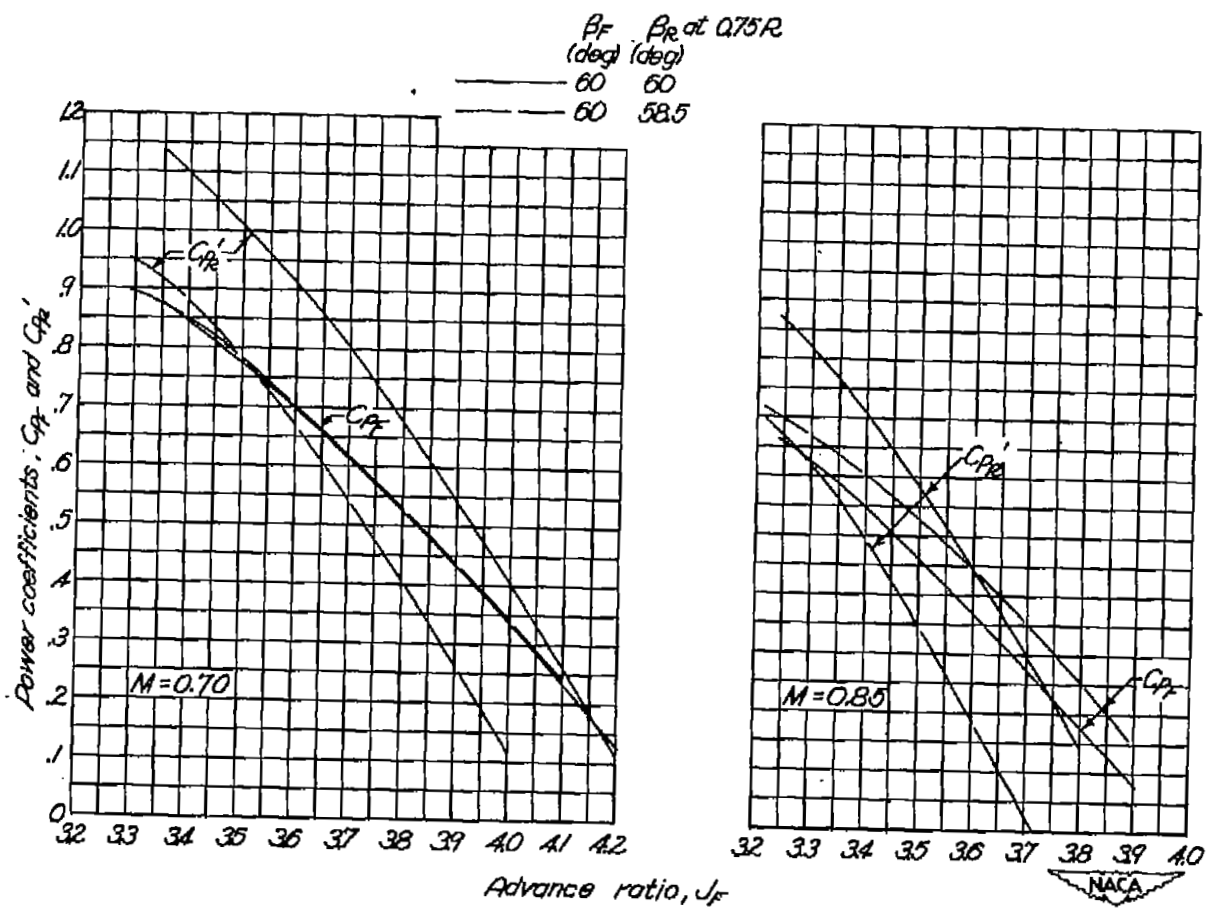
(a) Individual power coefficients.

Figure 10.- Effect of small variations in rear blade angle for a front blade angle of 75° .



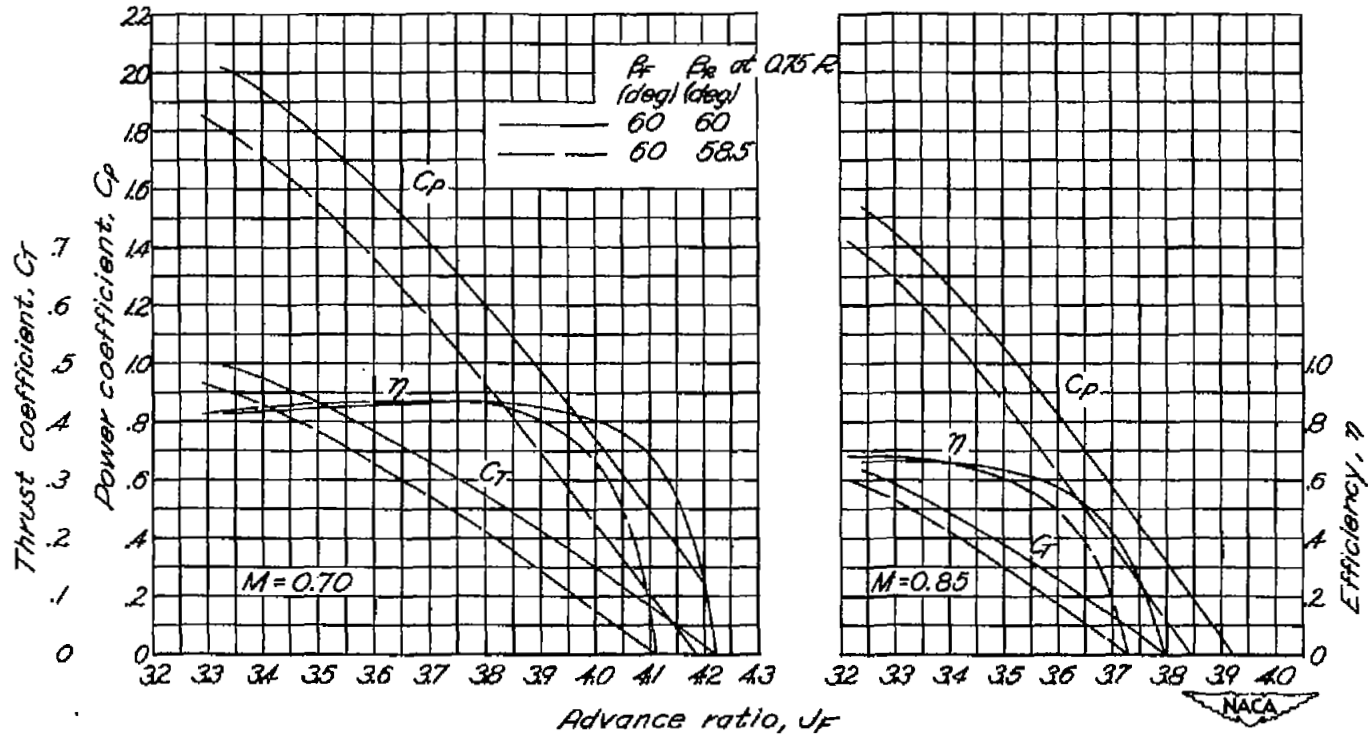
(b) Over-all propeller characteristics.

Figure 10.- Concluded.



(a) Individual power coefficients.

Figure 11.- Effect of small variations in rear blade angle for a front blade angle of 60°.



(b) Over-all propeller characteristics.

Figure 11.- Concluded.